Nanomanufacturing
University of Michigan
ME599-002 | Winter 2010

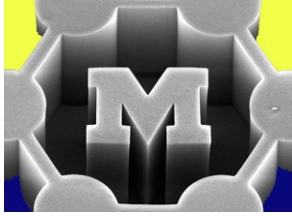

19: **Self-assembly and deposition of molecular monolayers**

March 31, 2010

John Hart
ajohnh@umich.edu
http://www.umich.edu/~ajohnh

Announcements

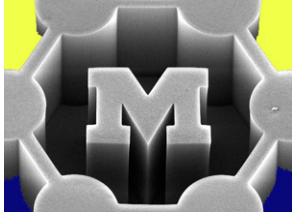

- Peer reviews due Friday
- Sign up for a 15 minute meeting with John
  - Thursday 4-6 PM or Sunday 1-3 PM, 2278 GGB
  - http://bit.ly/cBNAxk
  - If you don't have a team, list your name in **"looking for a team"** at the link above, and contact others
  - Meeting will focus on
    - Definition of key idea
    - Proposed details/feasibility of the idea
    - Expected analysis based on course material
    - Anything else..
  - If possible your entire team should attend
  - Off-campus by phone

- **No lecture next Wednesday (Apr/7)**

Recap: self-assembly of micelles

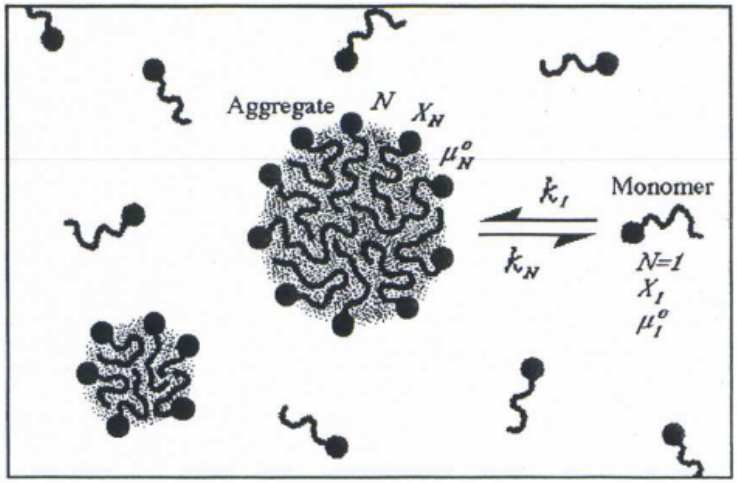

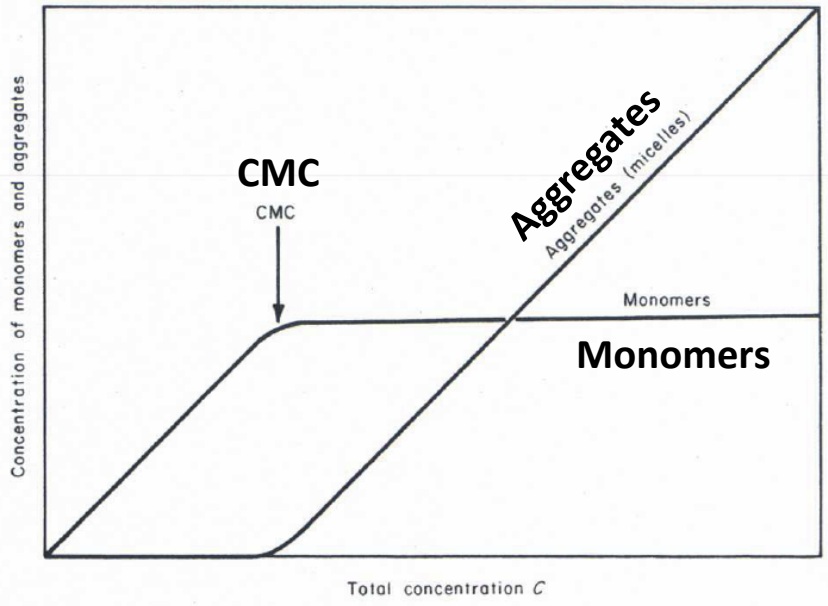

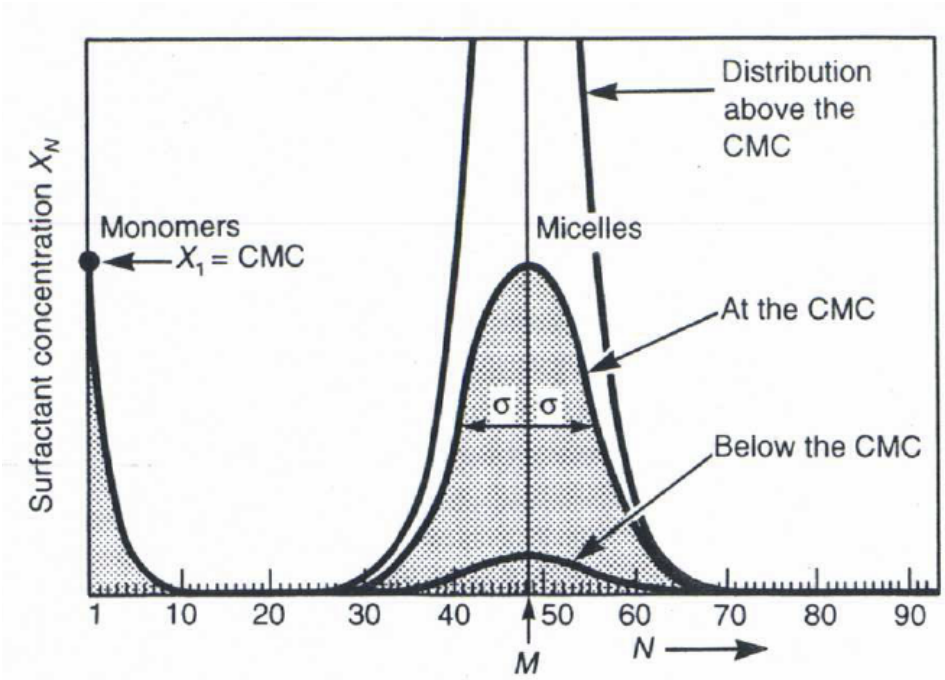

Israelachvili.

Block copolymers (BCPs)

- Chain of two chemically distinct polymer blocks, which are thermodynamically incompatible, e.g., repel each other
- Chains often must adopt extended configurations (i.e., not bunched) to keep dissimilar portions apart

Diblock

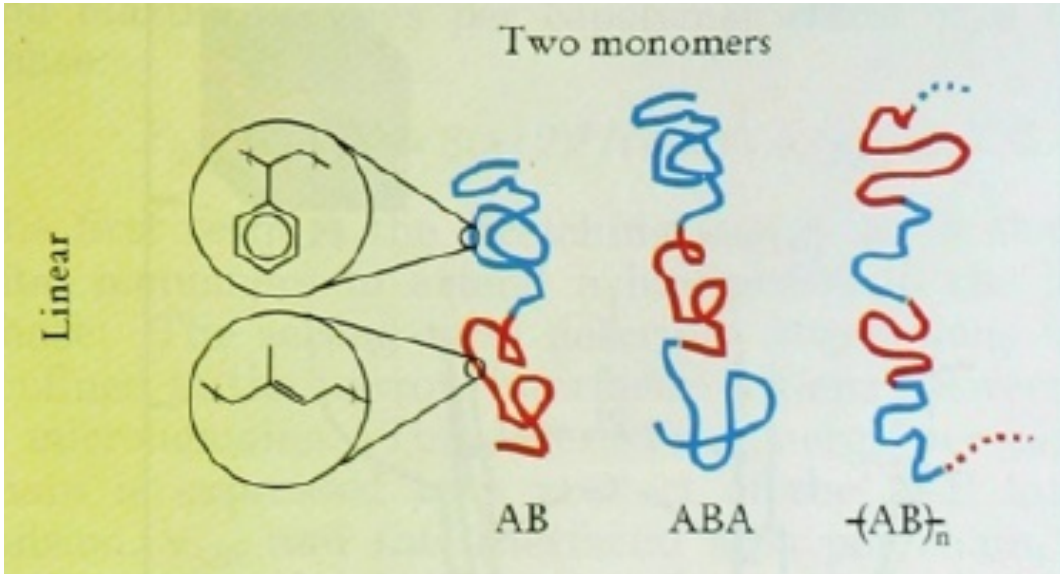

- e.g., PS-b-PMMA = polystyrene-b-poly(methyl methacrylate)
- usually made by first polymerizing styrene, and then subsequently polymerizing MMA from the reactive end of the polystyrene chains

Bates and Fredrickson, *Physics Today* February 1999, p. 32-38.

Self-assembly by phase separation

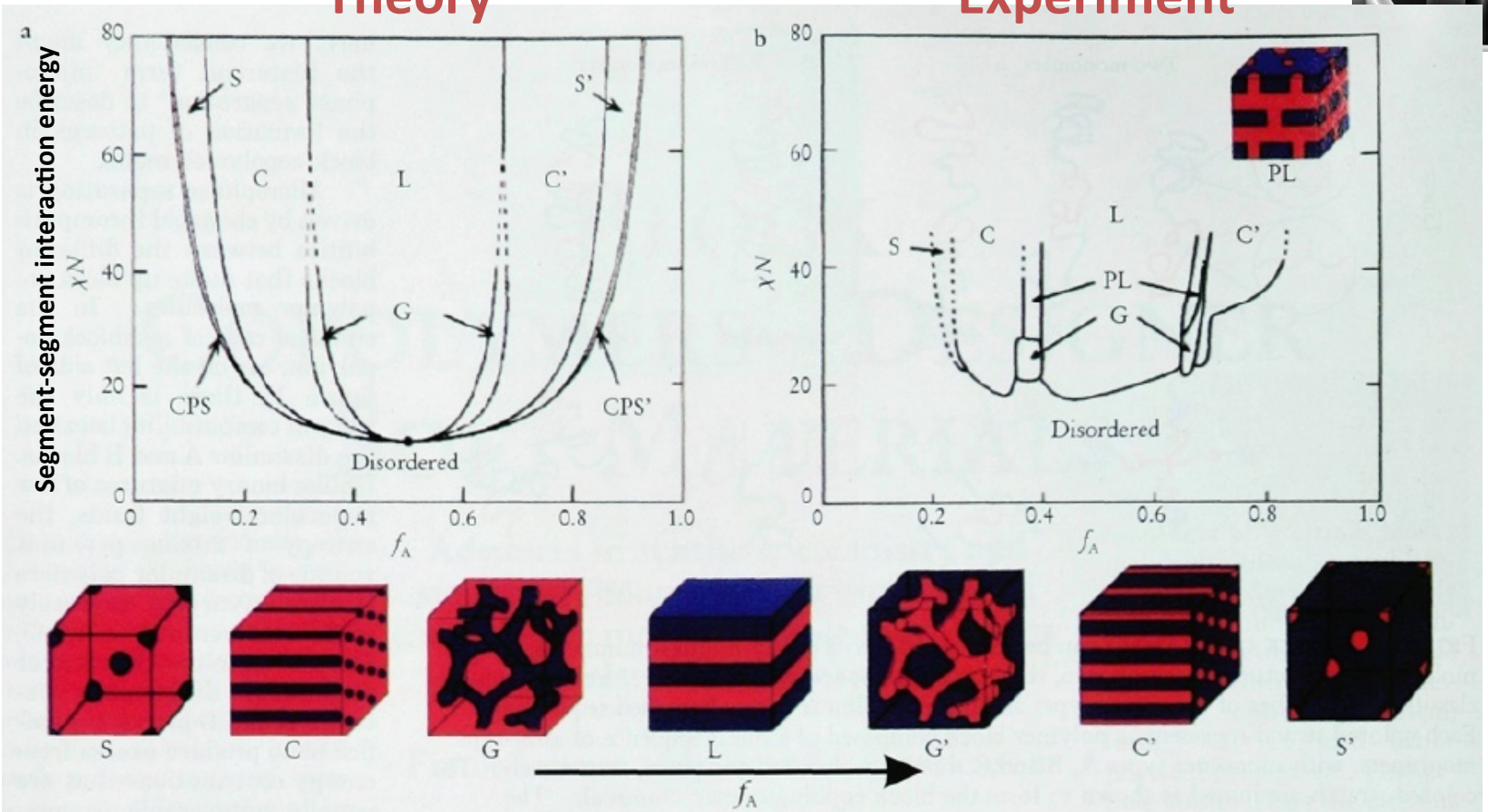

FIGURE 3. PHASE DIAGRAM for linear AB diblock copolymers, comparing theory and experiment. **a:** Self-consistent mean-field theory[8] predicts four equilibrium morphologies: spherical (S), cylindrical (C), gyroid (G) and lamellar (L), depending on the composition f and combination parameter χN. Here, χ is the segment–segment interaction energy (proportional to the heat of mixing A and B segments) and N is the degree of polymerization (number of monomers of all types per macromolecule). **b:** Experimental phase portrait for poly(isoprene-styrene) diblock copolymers.[9] The resemblance to the theoretical diagram is remarkable, though there are important differences, as discussed in the text. One difference is the observed PL phase, which is actually metastable. Shown at the bottom of the figure is a representation of the equilibrium microdomain structures as f_A is increased for fixed χN, with type A and B monomers confined to blue and red regions, respectively.

Bates and Fredrickson, *Physics Today* February 1999, p. 32-38.

SEM images of diblock gyroid network

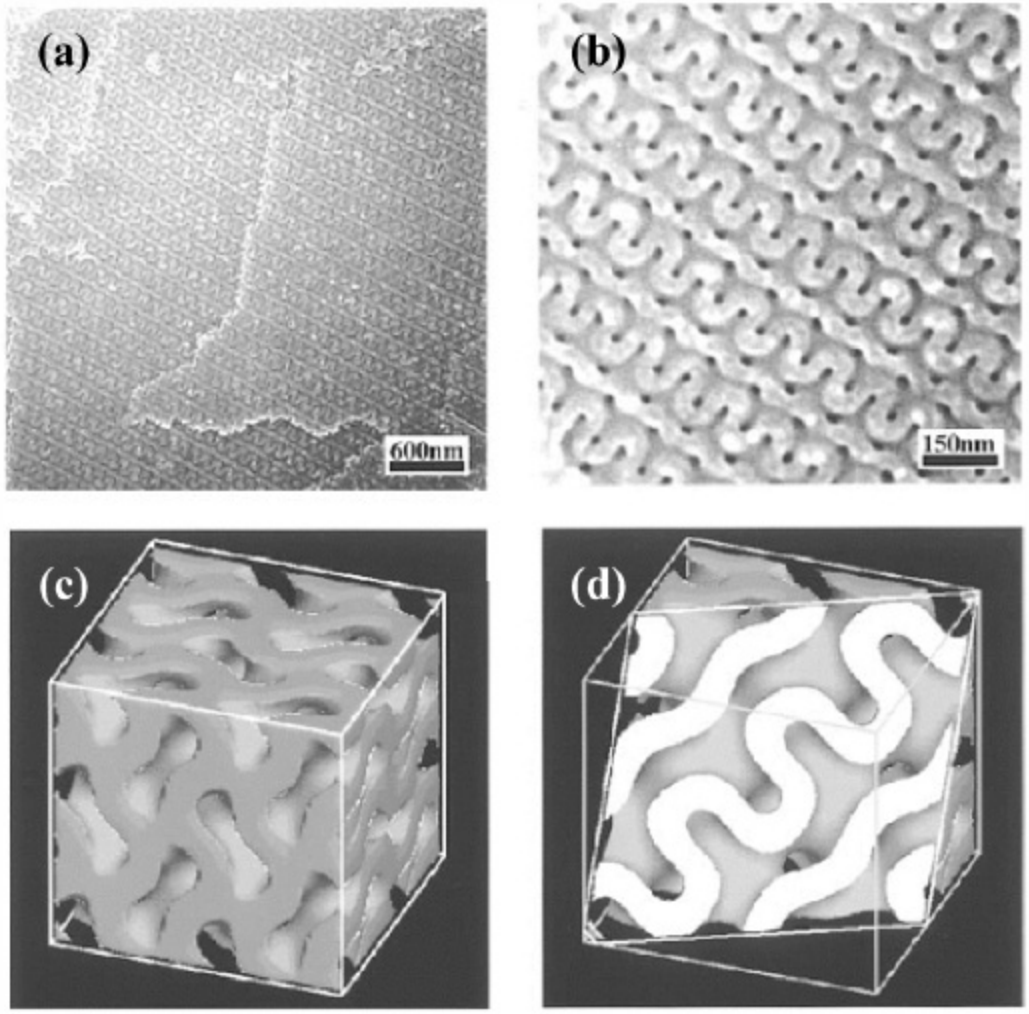

Fig. 2. SEM micrographs showing a bicontinuous nanochannel in the matrix of PS with two different magnifications ((a), (b)) and computer graphics of a double gyroid network: (c) a 3D view and (d) a 2D intersection cut along the (211) direction. (c) shows a solid model in which only the matrix phase, corresponding to the PS matrix in our specimens, is shown. In (d), the bright domain corresponds to the PS matrix and the gray and dark phases correspond to the degraded PI phase. (Reprinted with permission from *Langmuir* [42]. Copyright (1997) American Chemical Society).

Park et al. *Polymer* 44:6725-6760, 2003.

Templated self-assembly of BCPs

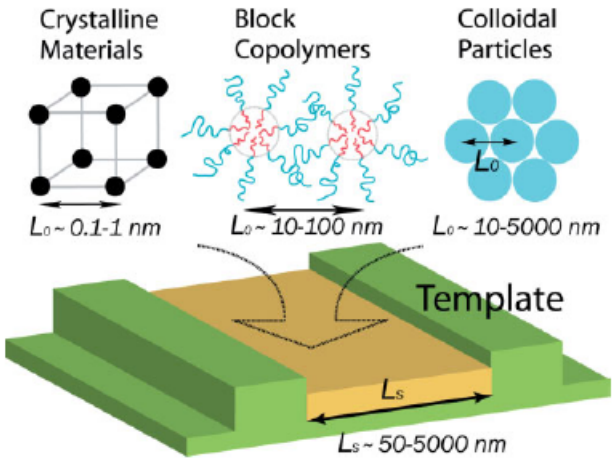

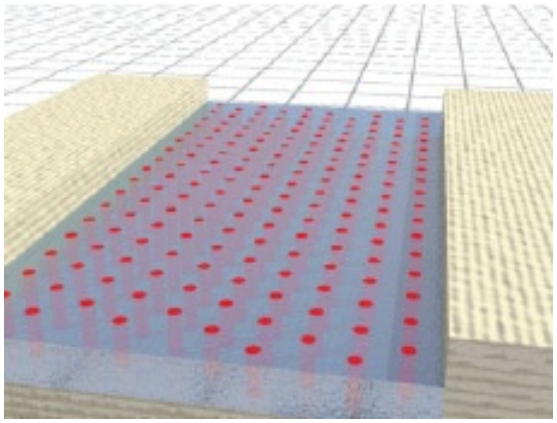

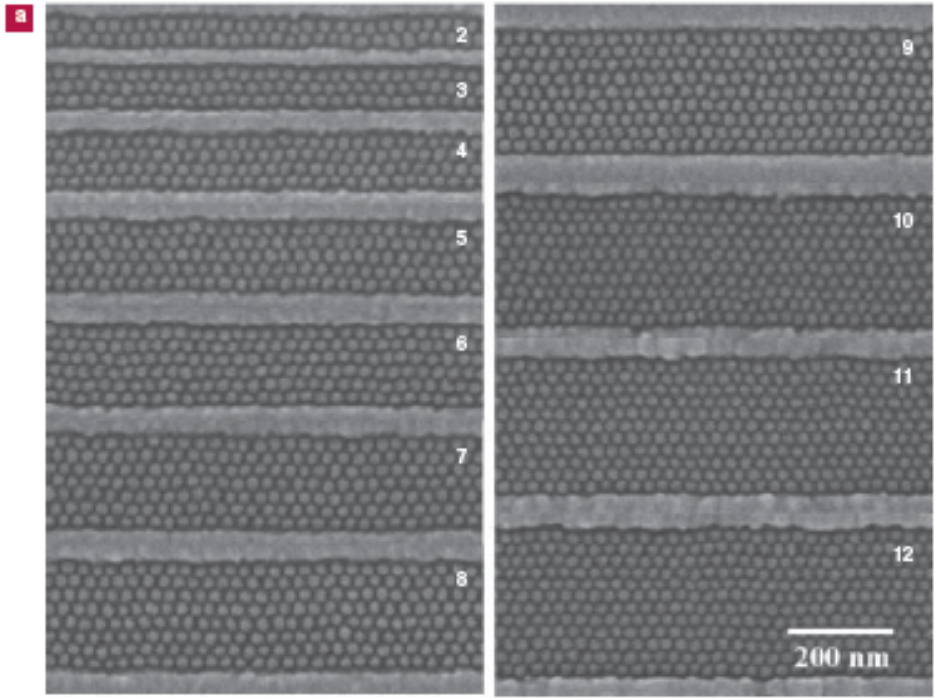

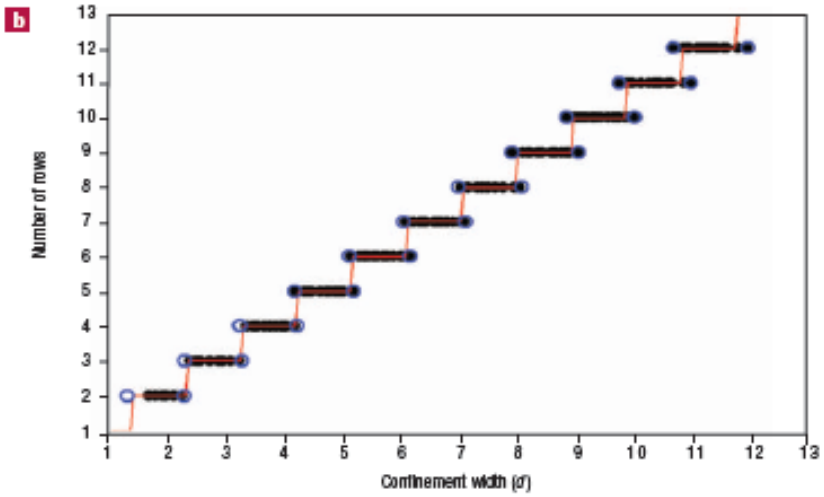

Cheng et al., *Nature Materials* 3:823-828, 2004.

BCP films as etch masks

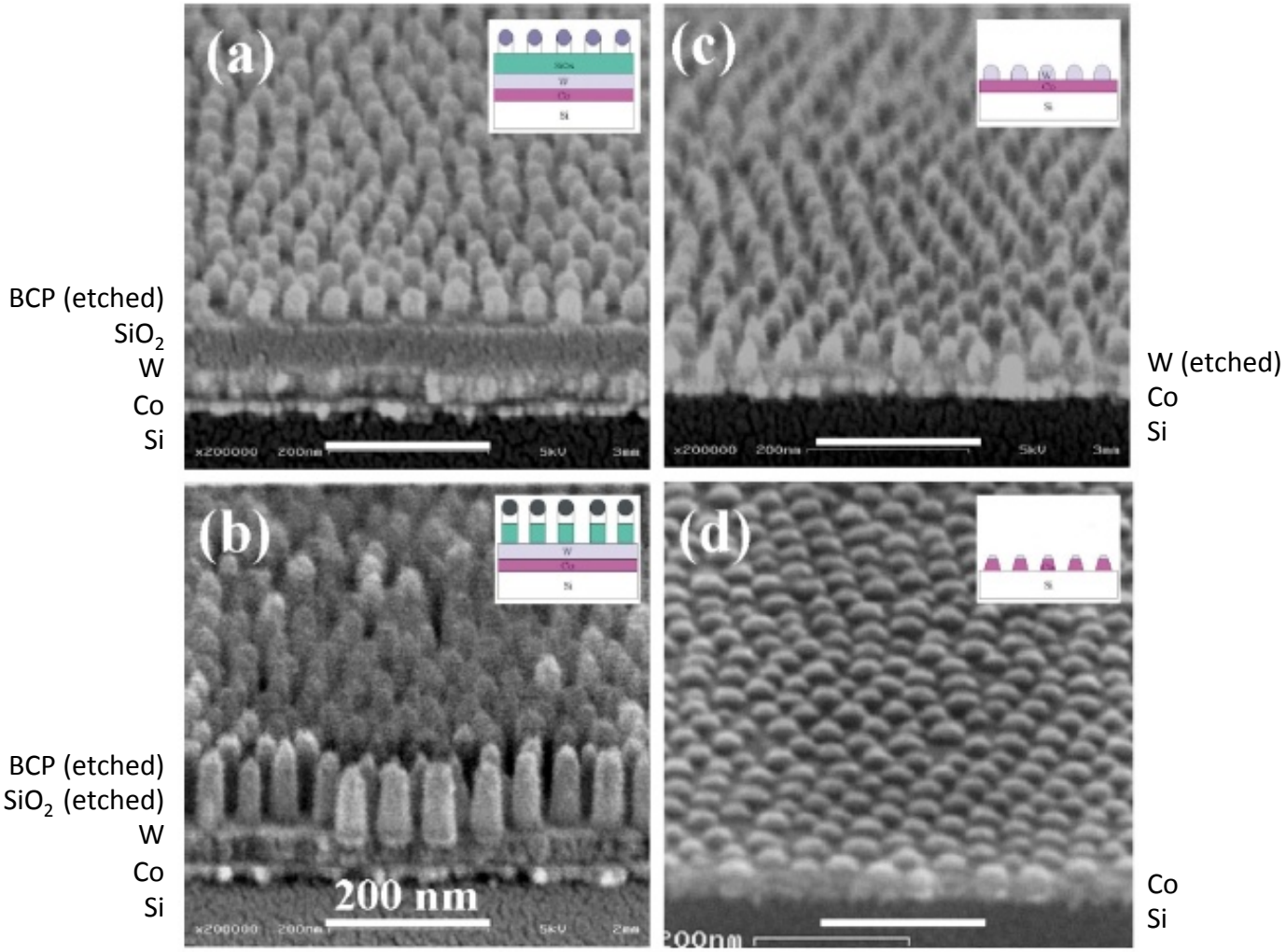

BCP (etched)
SiO_2
W
Co
Si

W (etched)
Co
Si

BCP (etched)
SiO_2 (etched)
W
Co
Si

Co
Si

Fig. 7. Tilted SEM micrographs of the fabrication process of Co dot array using PS-PFS BCPs. (a) An O_2-RIE treated block copolymer thin film on a multilayer of silica, the metallic films and the silicon substrate. (b) Pillars of silicon oxide capped with oxidized PFS after CHF_3-RIE. (c) W (tungsten) hard mask on top of a Co layer. (d) Co dot array produced Ne ion-beam etching. (Reprinted with permission from *Adv Mater* [91]. WILEY-VCH, STM-Copyright & Licenses (2001)).

Park et al. *Polymer* 44:6725-6760, 2003.

Ordered nanoparticle arrays by self-assembly: micellar solutions and block copolymer films

Like a nanoparticle-filled photoresist

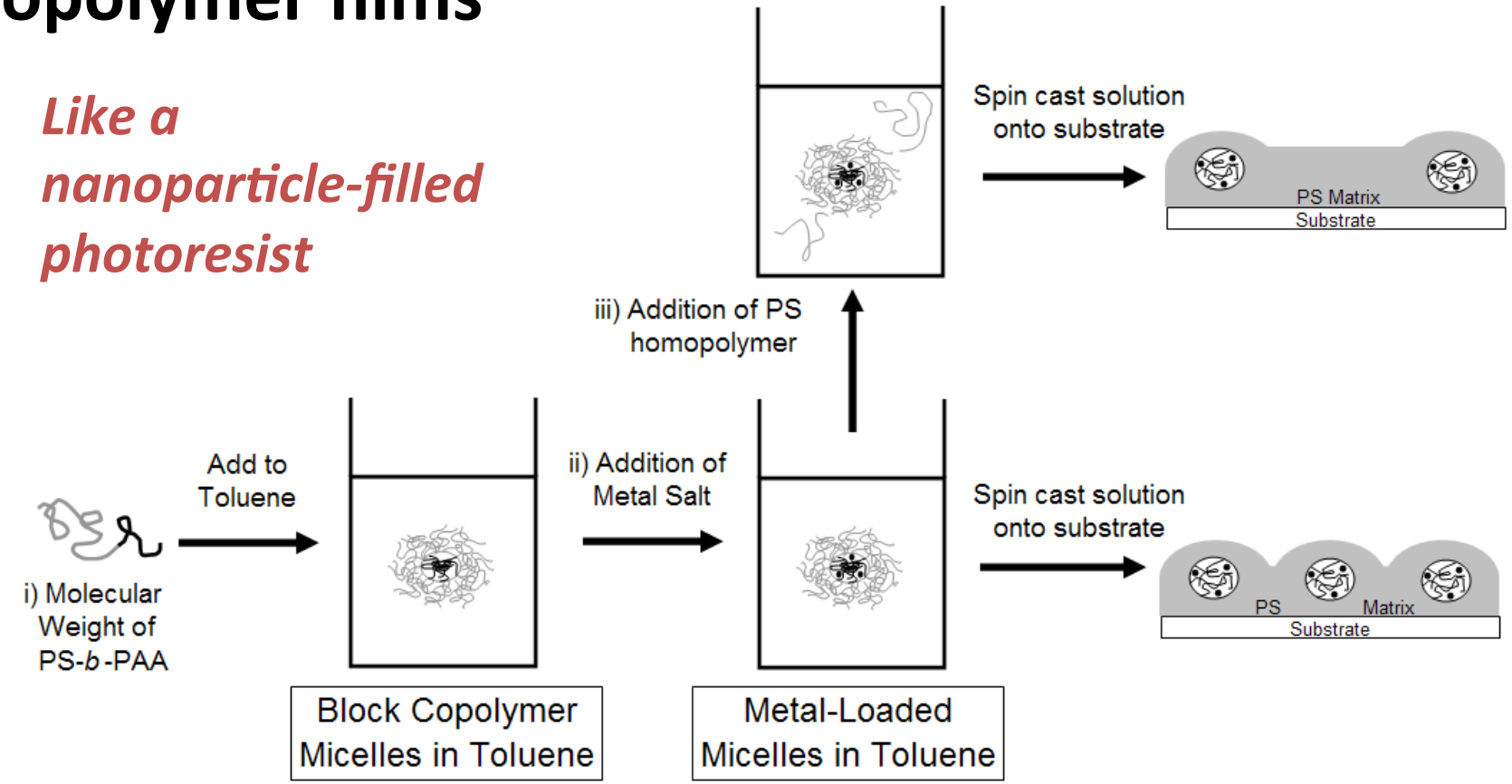

- **Micelle size = nanoparticle size**
- **Homopolymer chain length = particle spacing**

R. Bennett, R. Cohen, et al.

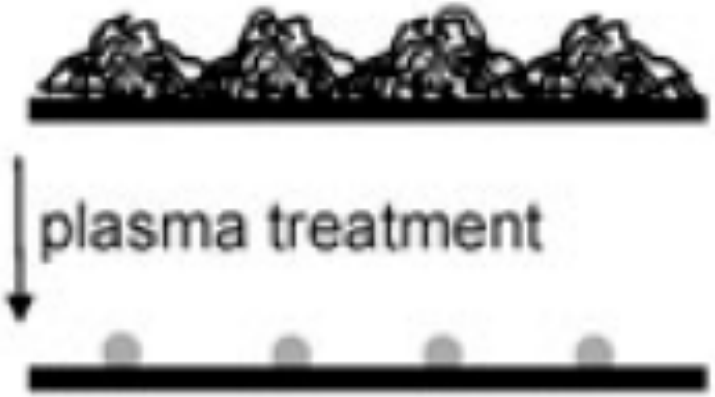

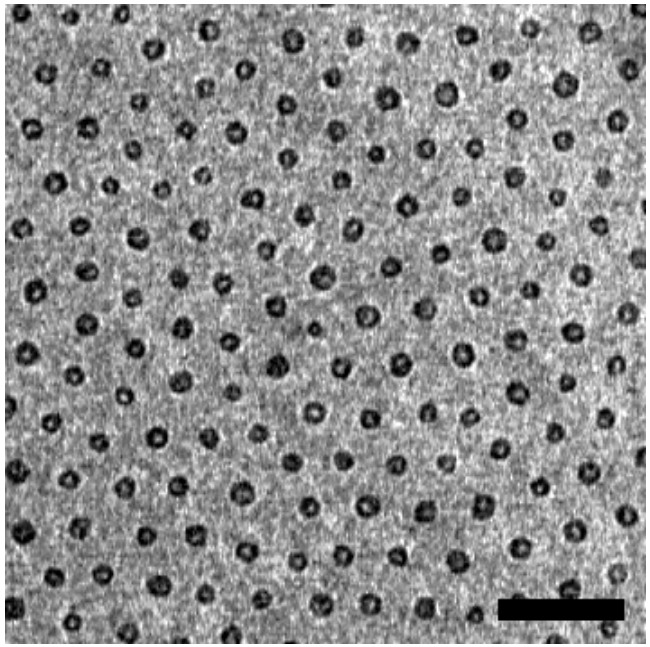

→ ***Independent control of size and spacing***

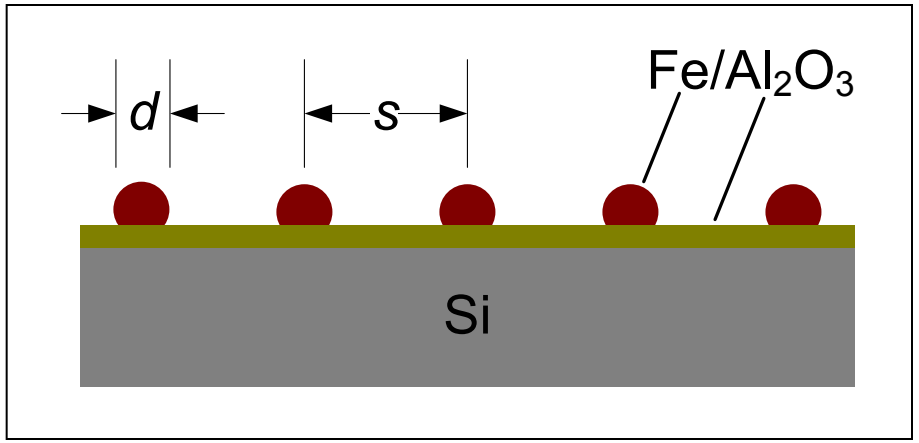

R. Bennett, R. Cohen, et al.

CNT film and forest growth from BCP-templated catalyst films

Q: What is the critical catalyst density for vertically aligned growth?

Before Growth

Particle diameter 16±2 nm

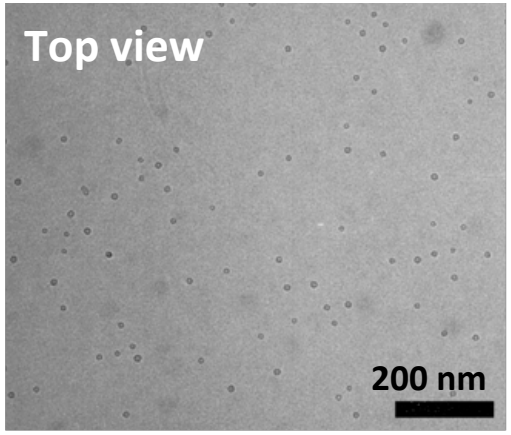

6×10^9 particles/cm^2

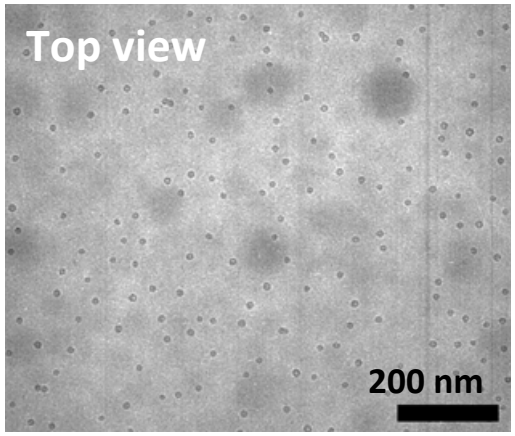

2.5×10^{10} particles/cm^2

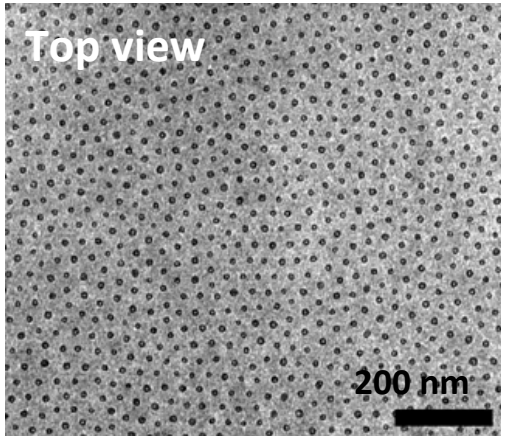

6×10^{10} particles/cm^2

After Growth

CNT diameter 12±2 nm, 8 walls

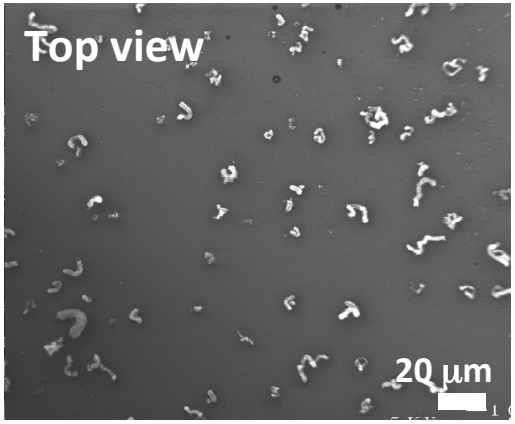

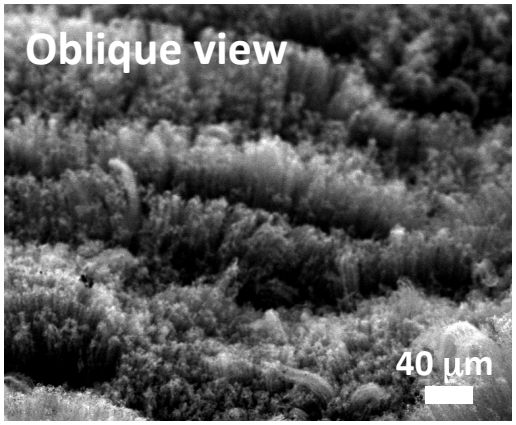

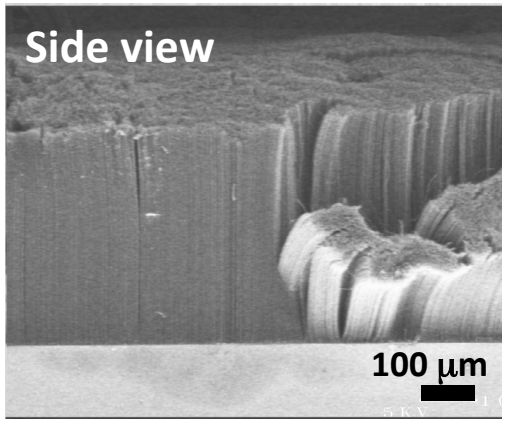

but only ≈5% activity!

Morphology control: Bennett, Hart, Cohen, *Advanced Materials* 18:2274-9, 2006.
Micro-contact printing: Bennett, Hart, et al., *Langmuir* 22:8273-8276, 2006.

BCP films as templates

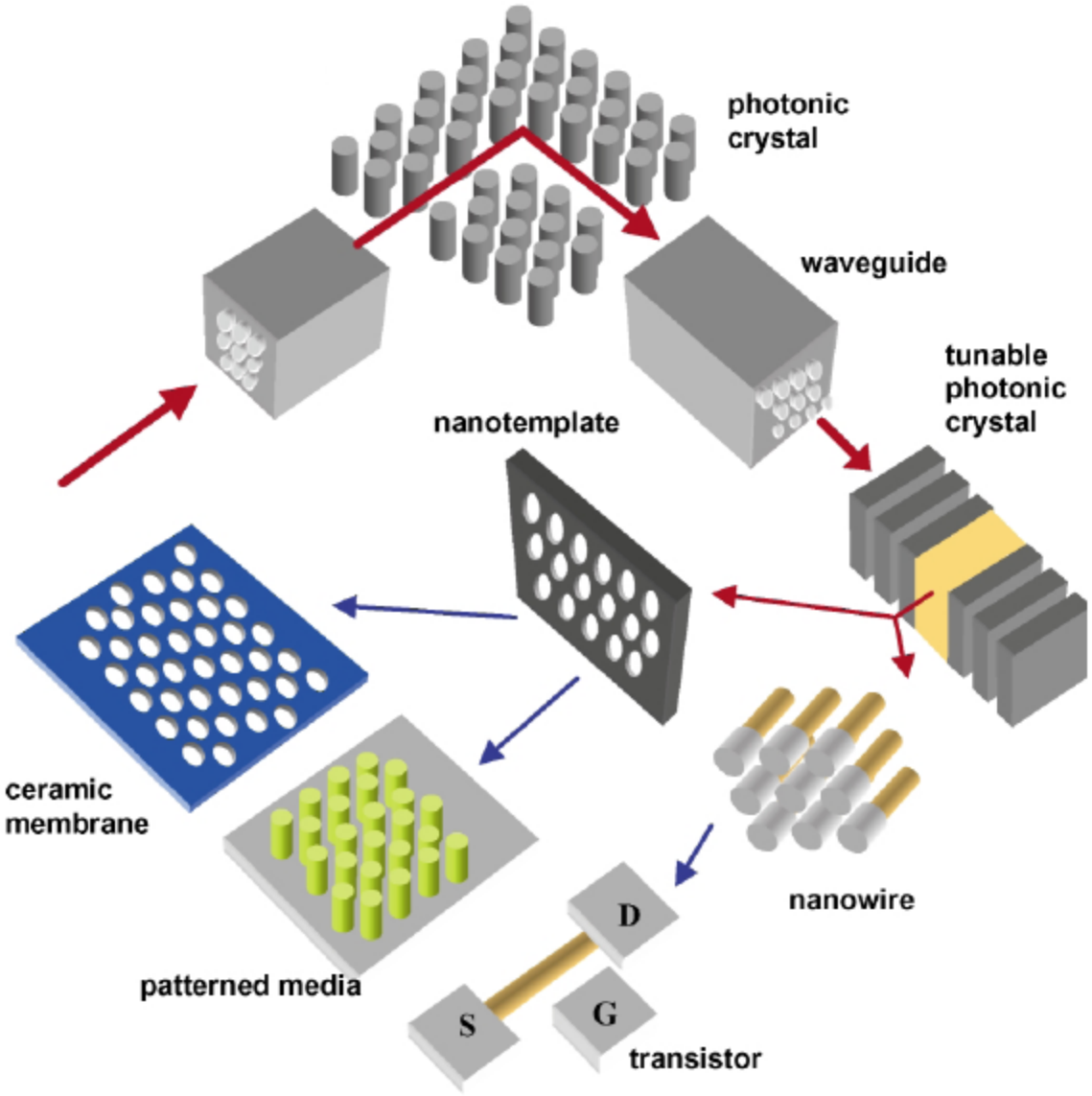

Park et al. *Polymer* 44:6725-6760, 2003.

Assembly of BCPs on SWNTs

- Interplay between BCP phase separation and CNT-induced crystallization of polyethylene (PE)

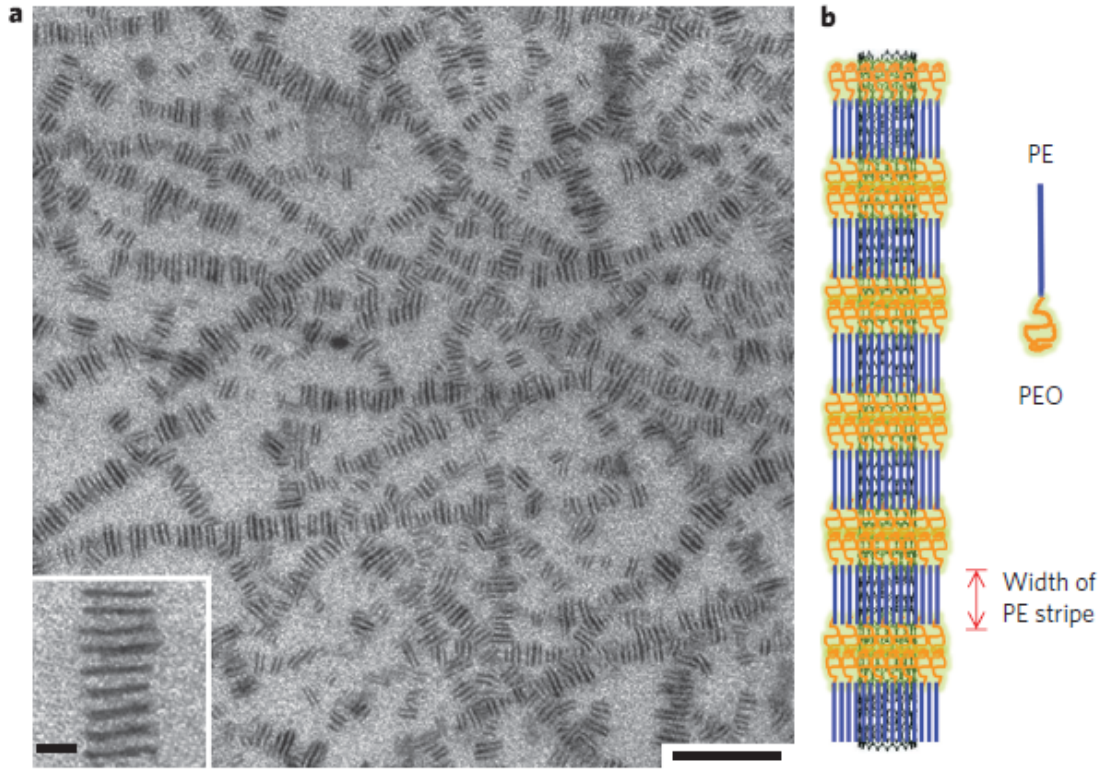

Figure 1 | The alternating pattern of PE-*b*-PEO block copolymers formed on SWNTs. a, TEM image of the PE-*b*-PEO decorated SWNTs. The dark and bright stripes are the PEO and PE domains, respectively. The formation of this unique structure is attributed to the subtle interplay between carbon nanotube-induced polymer crystallization and block copolymer phase separation (scale bar, 200 nm). The inset shows an enlarged area (scale bar, 20 nm). **b**, Schematic representation of the arrangement of the PE-*b*-PEO molecules along a SWNT.

Li et al., *Nature Nanotechnology* 4:358-362, 2009.

Mechanism and kinetics

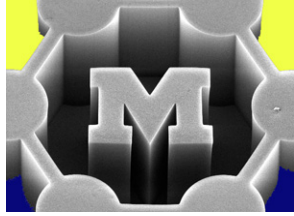

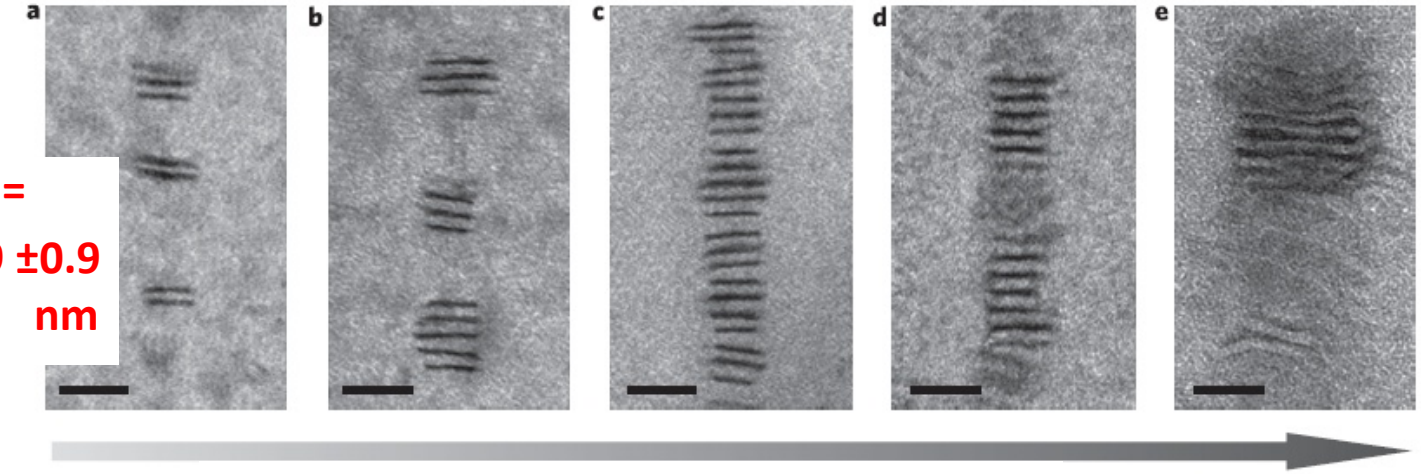

Period = 11.9 ±0.9 nm

Increasing concentration

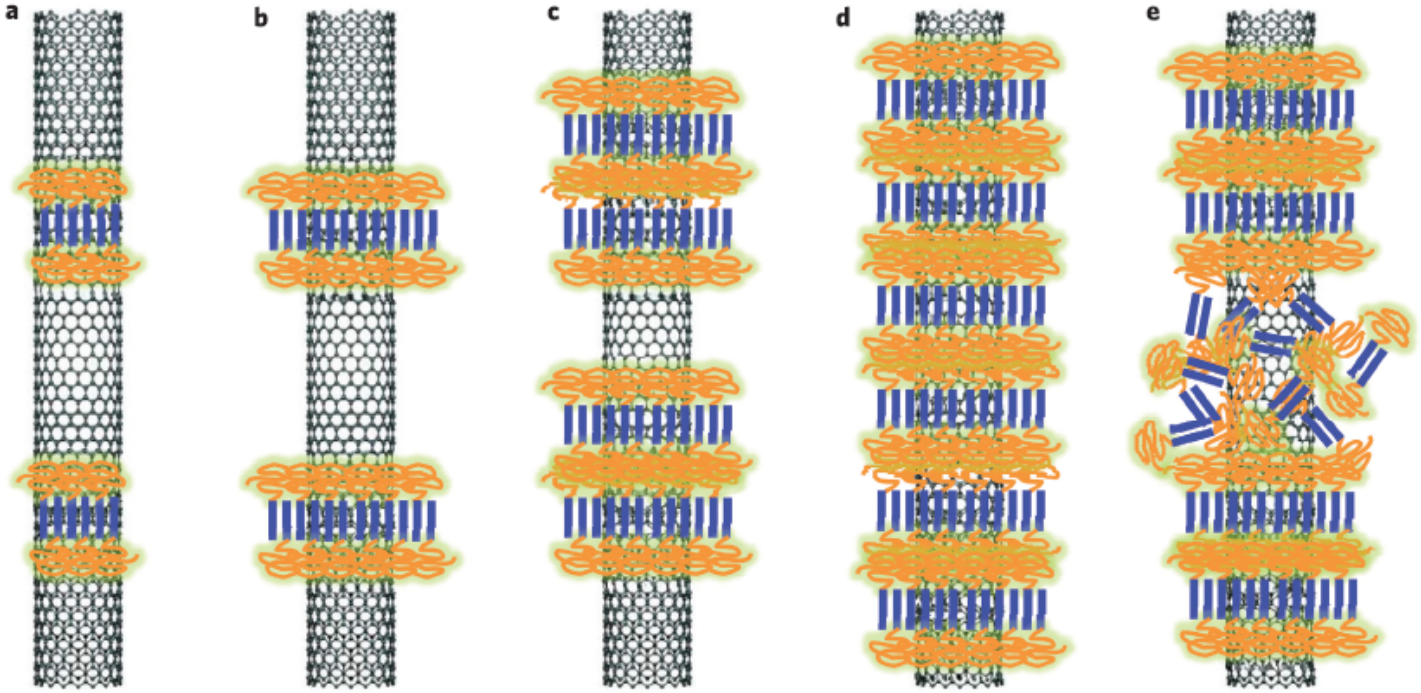

Concentration too high, not enough time for full crystal growth

Li et al., *Nature Nanotechnology* 4:358-362, 2009.

Anchoring Au NPs to BCPs on SWNTs

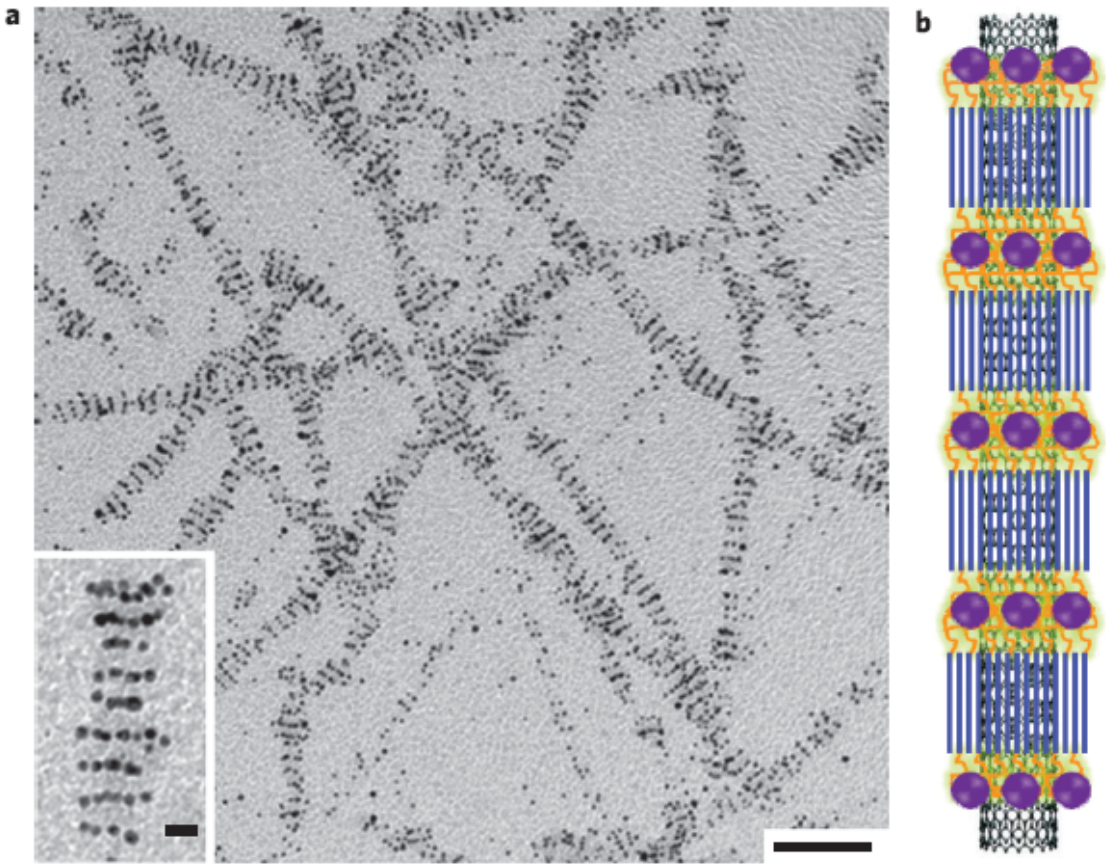

Figure 4 | Periodic immobilization of 5-nm gold nanoparticles on the block copolymer/SWNT hybrid. a, TEM image of the gold nanoparticle-decorated block copolymer/SWNT hybrid. The block copolymer is end-functionalized with a thiol group (scale bar, 100 nm). The inset shows an enlarged area (scale bar, 10 nm). **b**, Schematic representation of the arrangement of the gold nanoparticles and the block copolymer chains along an SWNT.

Li et al., *Nature Nanotechnology* 4:358-362, 2009.

Triblock morphologies

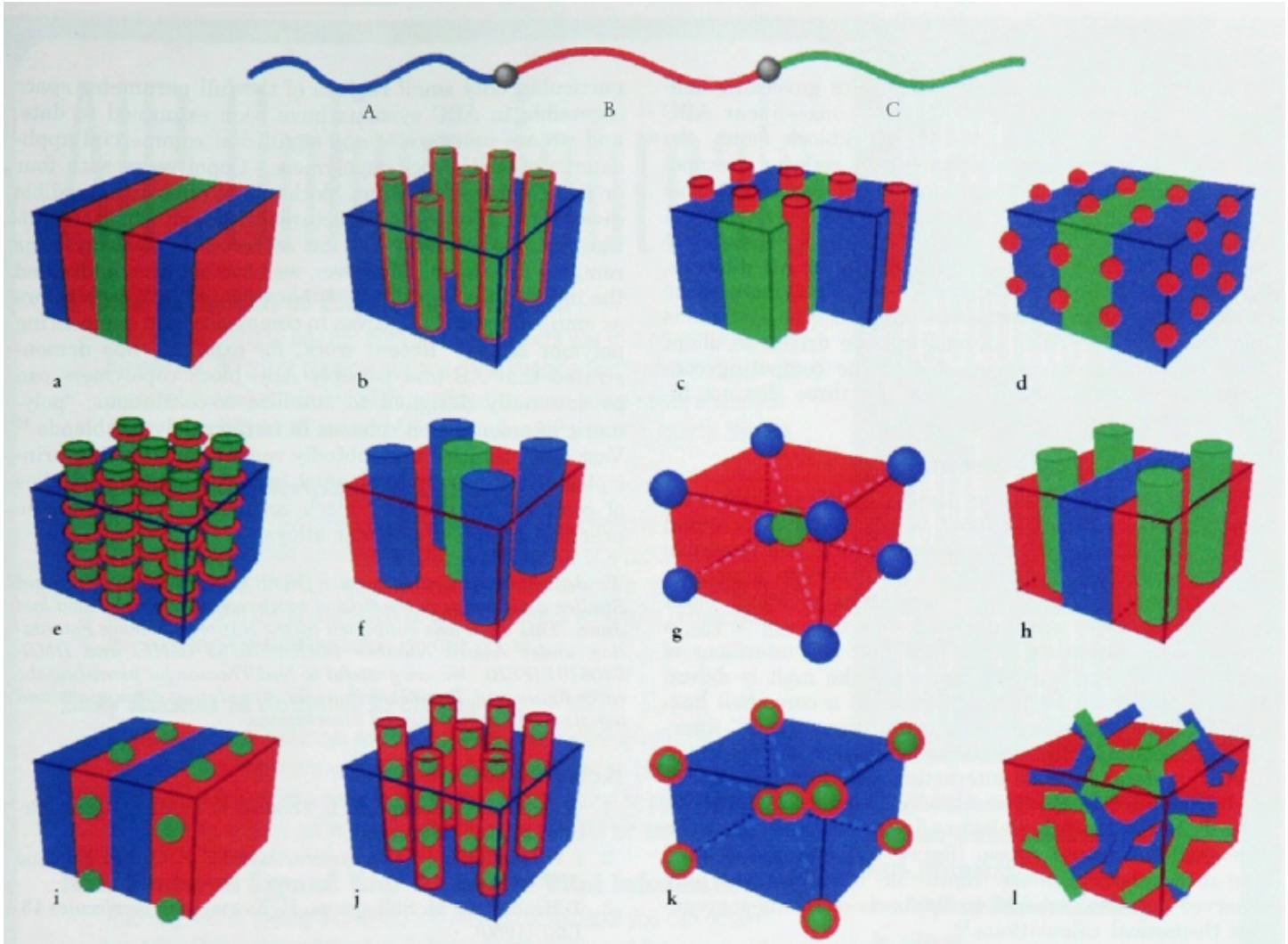

FIGURE 5. MORPHOLOGIES FOR LINEAR ABC triblock copolymers. A combination of block sequence (ABC, ACB, BAC), composition and block molecular weights provides an enormous parameter space for the creation of new morphologies. Microdomains are colored as shown by the copolymer strand at the top, with monomer types A, B and C confined to regions colored blue, red and green, respectively. (Adapted from Zheng and Wang in ref. 13.)

Bates and Fredrickson, *Physics Today* February 1999, p. 32-38.

From synthesis to assembly

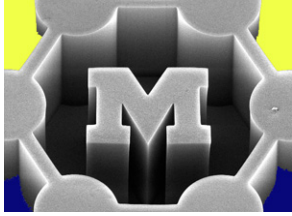

2D

- Film deposition and growth (physical/chemical):
  - growth of films of nanotubes/wires
  - monolayer self-assembly

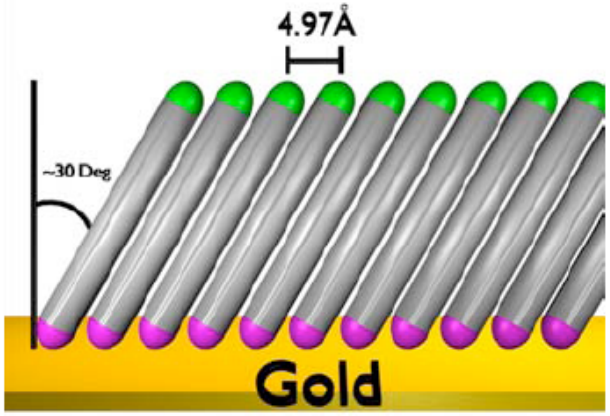

3D (all effects together)

- Colloidal crystals, superlattices
- Yarn spinning, networks, aerogels, composites, etc.

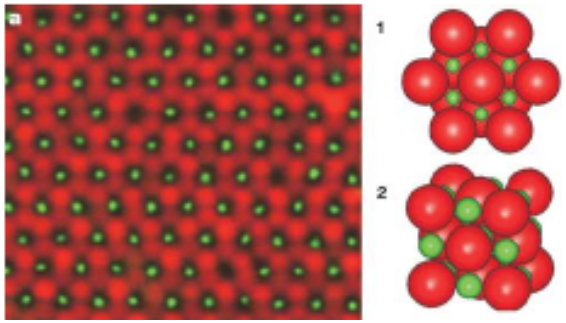

The goal is to maintain order as we scale up!

Reversibility is key to self-assembly

Interactions **balance** to give an equilibrium separation

Irreversible process is not self-assembly

Self-assembly Motion and reversibility = error-correction = **order**

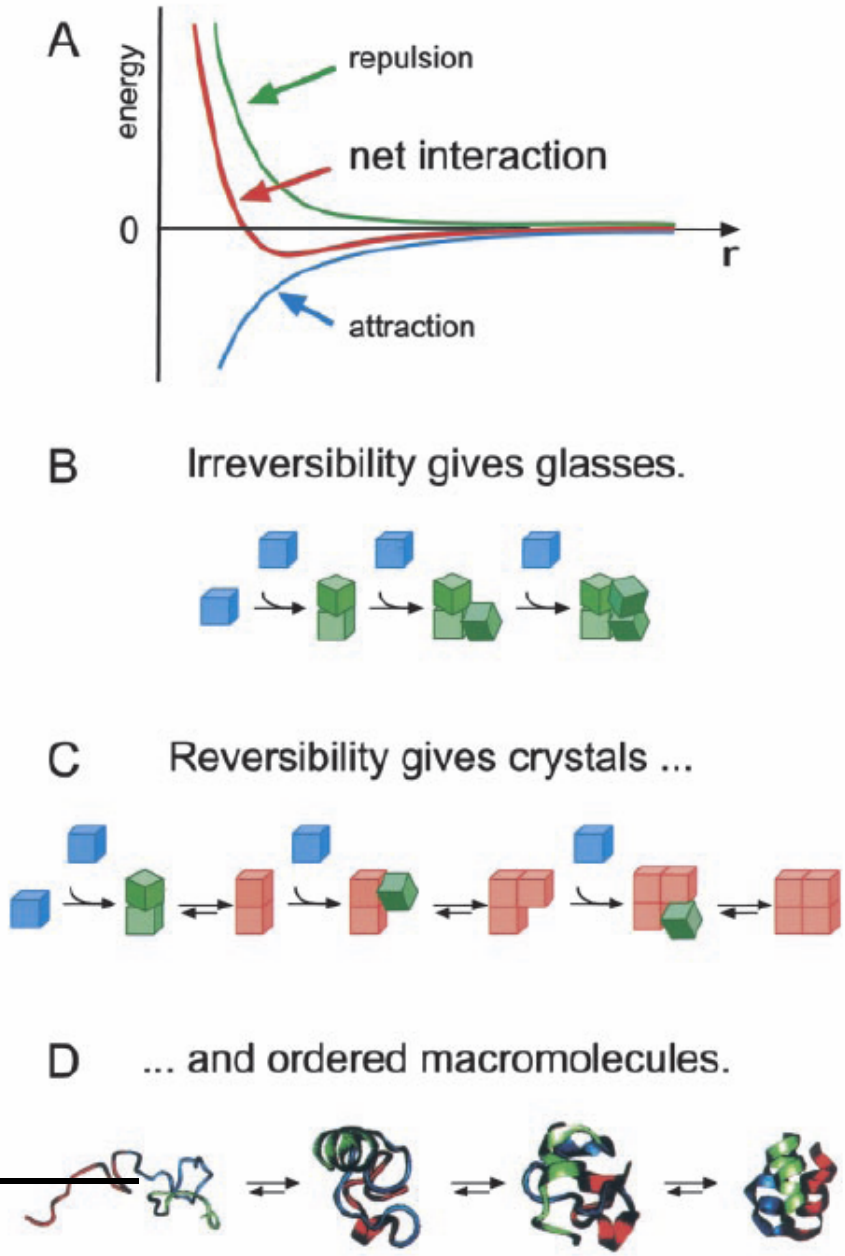

Fig. 1. (*A*) Aggregation occurs when there is a net attraction and an equilibrium separation between the components. The equilibrium separation normally represents a balance between attraction and repulsion. These two interactions are fixed in molecular self-assembly but can be engineered independently in macroscopic self-assembly. (*B* and *C*) Schematic illustration of the essential differences between irreversible aggregation and ordered self-assembly. (*B*) Components (shown in blue) that interact with one another irreversibly form disordered glasses (shown in green). (*C*) Components that can equilibrate, or adjust their positions once in contact, can form ordered crystals if the ordered form is the lowest-energy form (shown in red). (*D*) Biology provides many examples of self-assembly (here, the formation of a protein, an asymmetric, catalytically active nanostructure); these examples will stimulate the design of biomimetic processes.

Whitesides and Boncheva, *PNAS* 99(8):4769, 2002.

©2(

Monolayer: definition

A *single* (2D) layer of molecules on a surface

http://goldbook.iupac.org/M04015.html

*let's define a 2D layer as having **< 10 nm** thickness; typically a monolayer is 0.5-5 nm thick

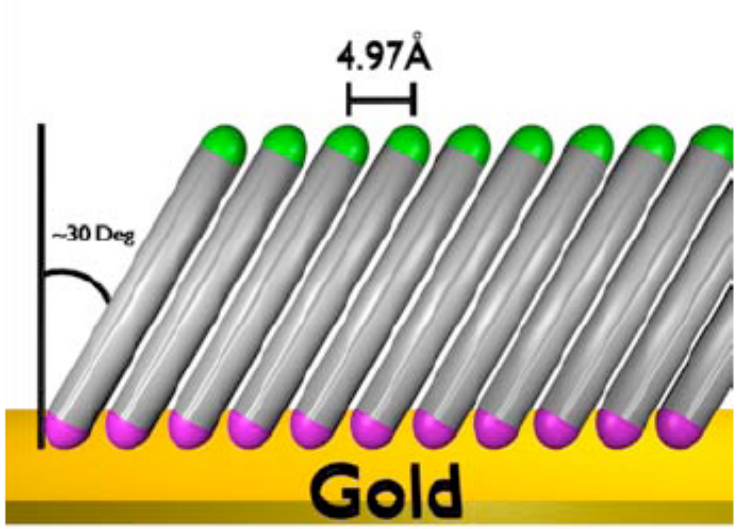

Today's agenda

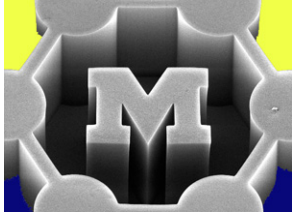

- Formation of self-assembled monolayers (SAMs)
- Deposition of SAMs by Langmuir-Blodgett methods

Today's readings

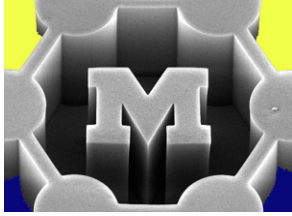

Nominal: (ctools)

- Asemblon Inc., "General introduction to self-assembled monolayers"
- Cote et al., "Langmuir-Blodgett assembly of graphene oxide single layers"

Extras: (ctools)

- Ulman, "Formation and structure of self-assembled monolayers"
- Blodgett (1935), "Films built by depositing successive monomolecular layers on a solid surface"

Self-assembled monolayer

A monolayer formed by (chemi)sorption on a surface submerged in a liquid

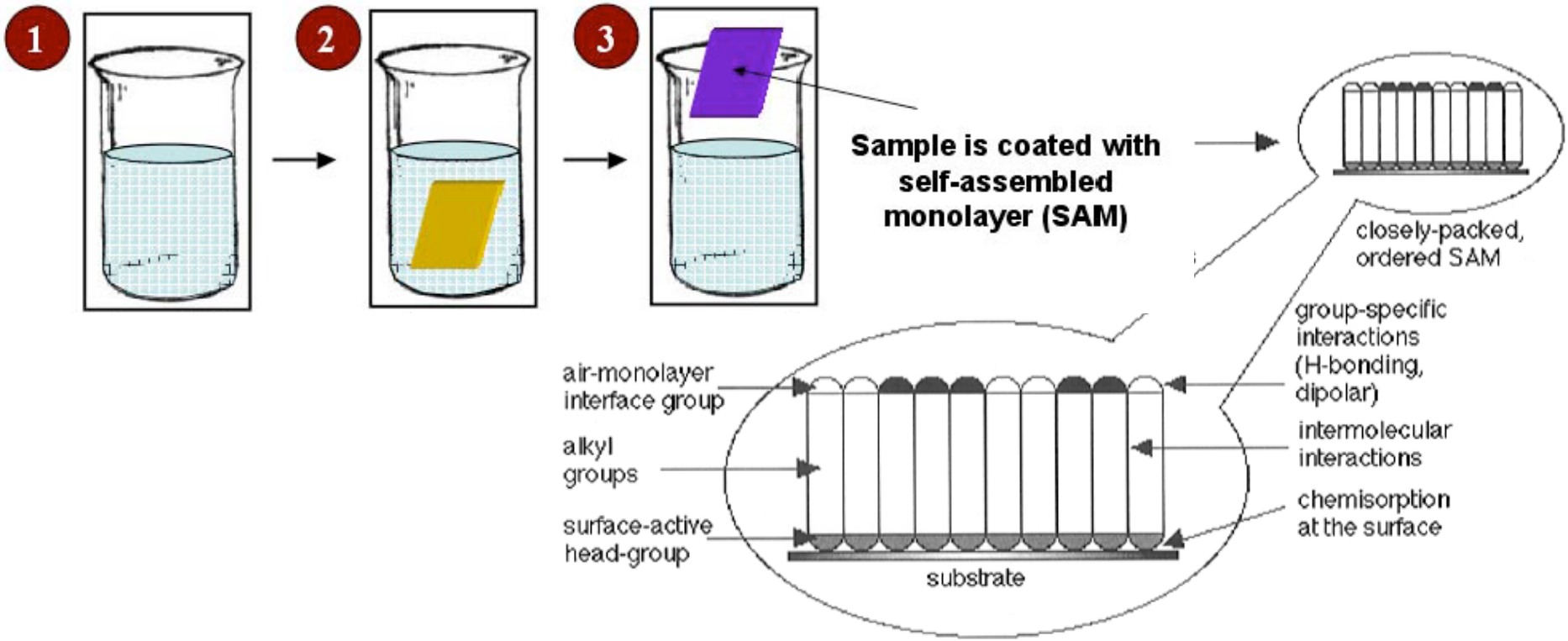

vs. physically-deposited films, SAMs are *highly ordered* and can incorporate direct *molecule design*. We can control effective surface properties by choosing the head group.

Ulman, *Chem. Rev.* 96:1533, 1996.

Chemisorbed vs. physisorbed

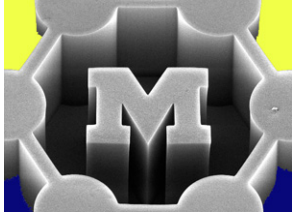

Chemisorption

- Molecule forms a chemical bond to surface
- High activation energy (strong)
- Low reversibility: etching or high temperature needed,e.g., catalysis

Physisorption

- Molecule attaches to substrate by VDW forces
- Low activation energy
- High reversibility: room temperature

→ *A dynamic process in kinetic equilibrium*

Molecule design

Amphiphile

Hydrophilic

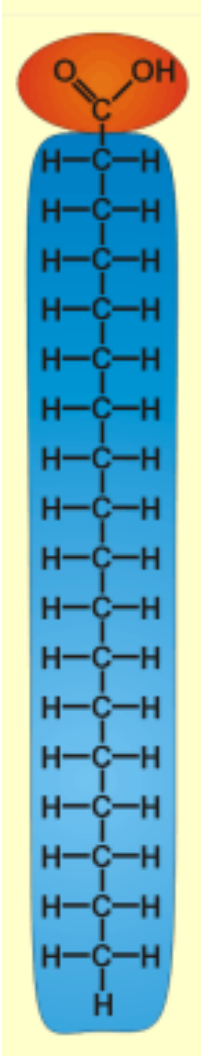

Hydrophobic

Alkanethiol on Au

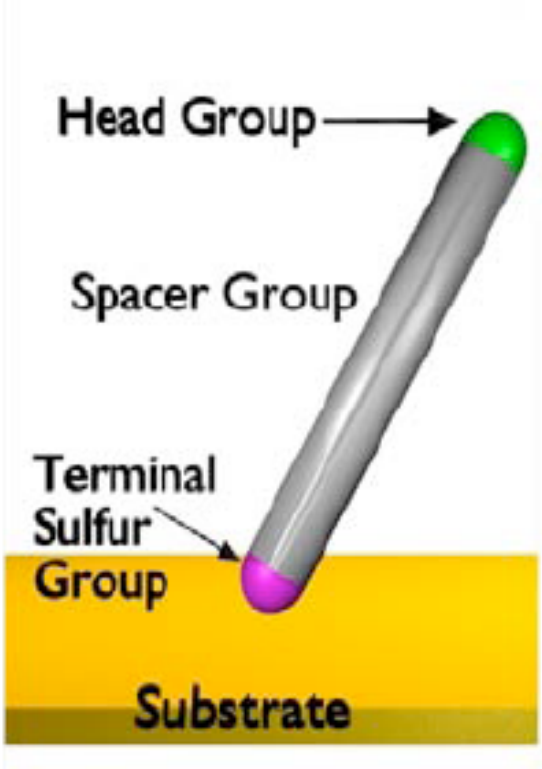

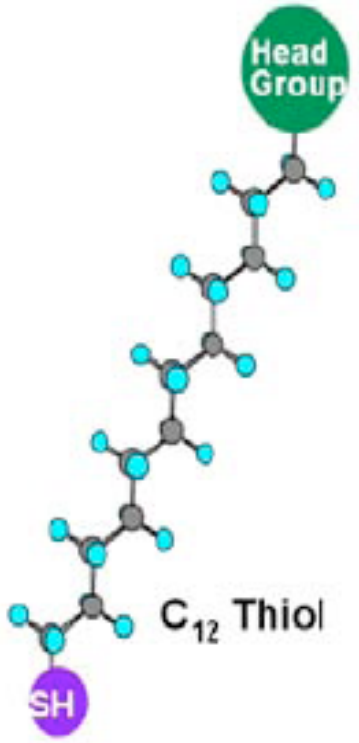

Head = for functionality
Body = for rigidity, length
Tail = match to surface

©2010 | A.J. Hart | 24

Configuration: balance between surface bonding and chain-chain interactions

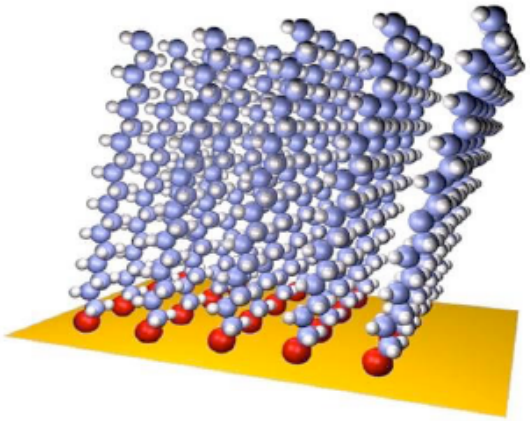

(fatty acid molecules)

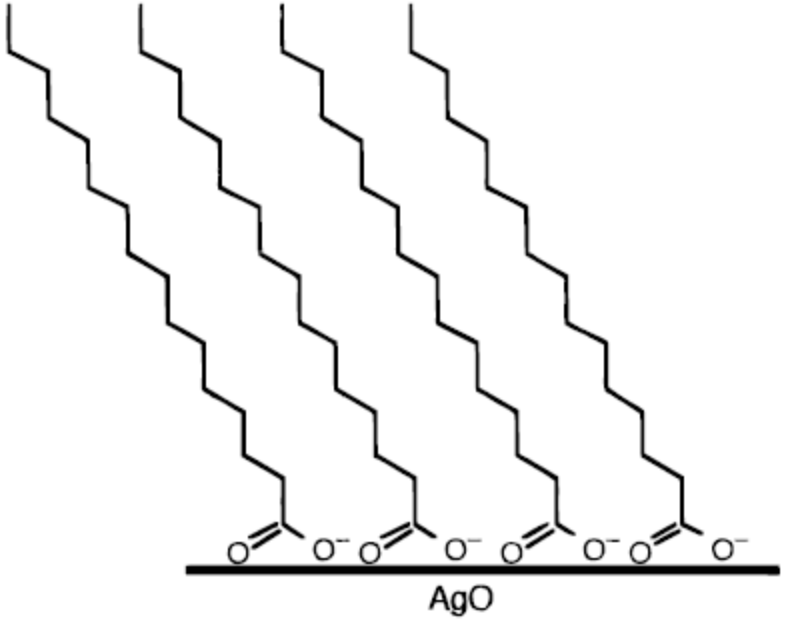

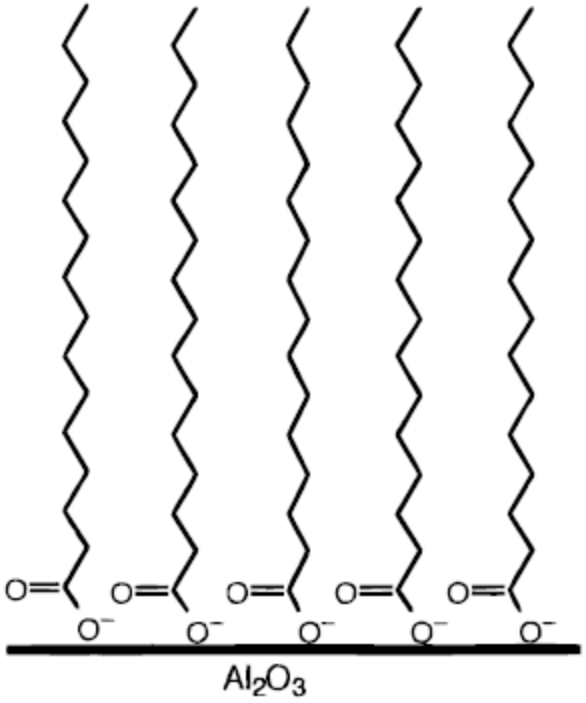

Ulman, *Chem. Rev.* 96:1533, 1996.

Siloxanes react with OH-terminations on metal and semiconductor surfaces (e.g., Si, SiO_2, ZnSe, mica, Au)

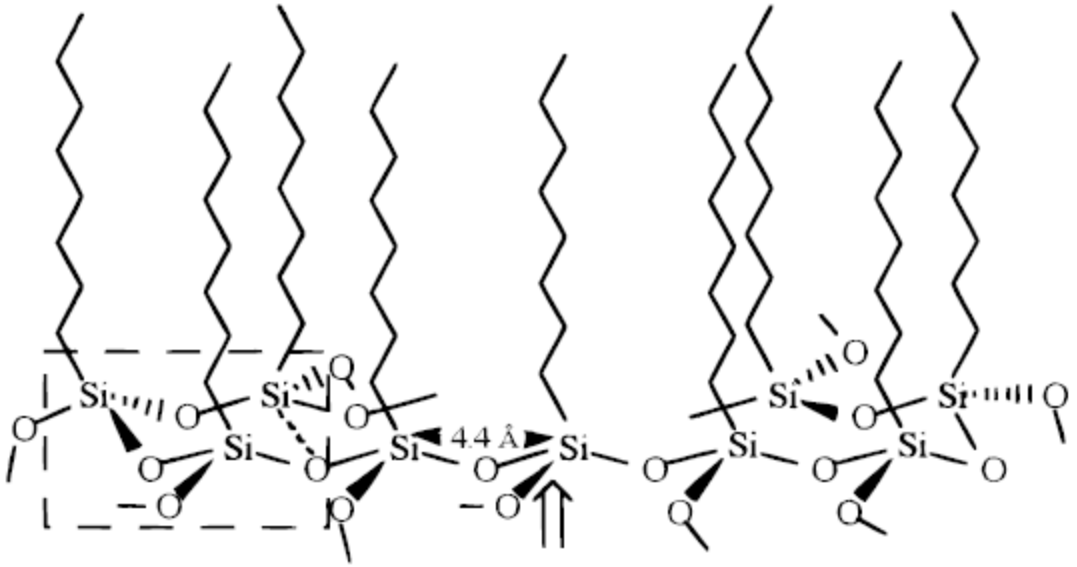

Figure 4. A schematic description of a polysiloxane at the monolayer–substrate surface. The arrow points to an equatorial Si–O bond that can be connected either to another polysiloxane chain or to the surface. (Adapted from Ulman, A., ref 1. Copyright 1991 Academic Press.) The dotted line on the left is a bond in a possible precursor trimer.

Pro: strong bonds

Con: low reversibility = poor long-range order

Ulman, *Chem. Rev.* 96:1533, 1996.

Kinetics of SAM formation

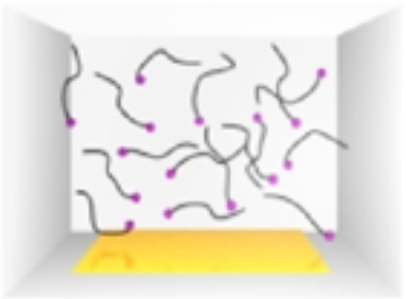

T = 0

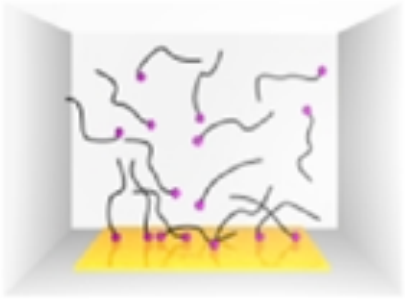

T = seconds

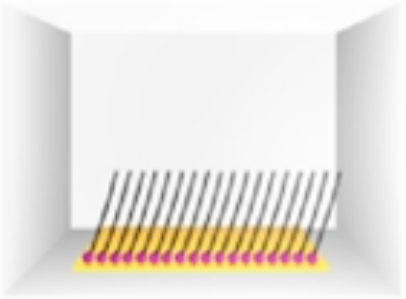

T = minutes to hours

"Annealing"

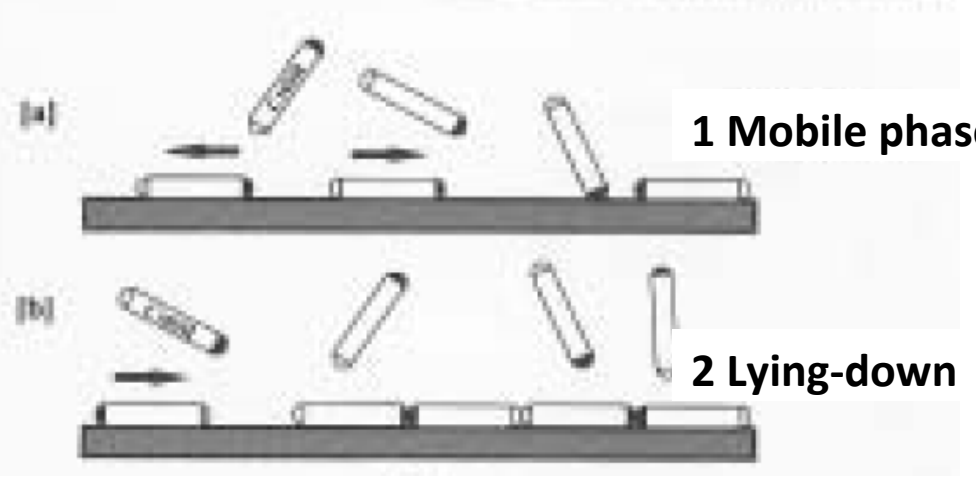

1 Mobile phase

2 Lying-down

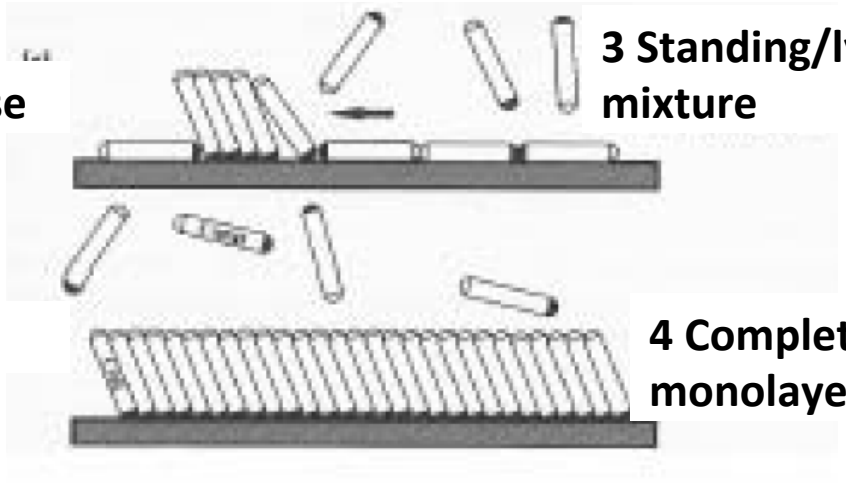

3 Standing/lying mixture

4 Complete monolayer

TABLE 1. Monolayers and multilayers formed by self-assembly on inorganic substrates.

MONOLAYERS

SURFACE	LIGAND	BINDING	REFERENCES
Au	RSH, ArSH (thiols)	RS–Au	27,30,36–42
Au	RSSR′ (disufides)	RS–Au	41,43
Au	RSR′ (sulfides)	RS–Au	44
SiO_2, glass	$RSiCl_3$,$RSiOR_3$	siloxane network	31,32,45–48
Si	$[RCOO]_2$ (neat)	R–Si	49
Si	$RCH{=}CH_2$, $[RCOO]_2$	$R{-}CH_2CH_2{-}Si$	50
GaAs	RSH	RS–GaAs	33–35
Ag	RSH, ArSH	RS–Ag	51–57
Cu	RSH, ArSH	RS–Cu	53,58–60
metal oxides	RCOOH	$RCO_2{-}\cdots MO_n$	61–73
metal oxides	RCONHOH	$RCONHOH\cdots MO_n$ $RCONHO{-}\cdots MO_n$	74,75
Pt	RSH, ArSH	RS–Pt	76–80
Pt	RNC	RNC–Pt	76

Langmuir isotherm

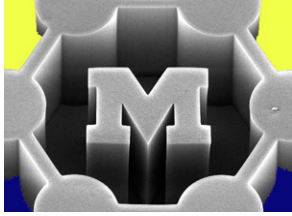

Increasing k_a/k_d
→ decreasing T
→ decreasing binding energy

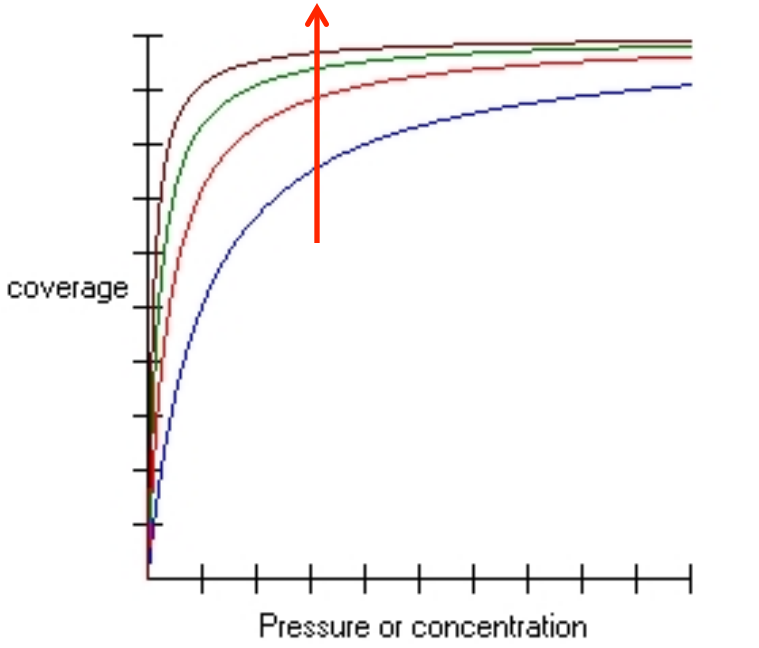

Monolayer adsorption

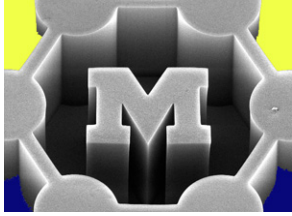

For a sticking coefficient of 1, STP
(perfect adsorption and no desorption)

$$t = 3 \times 10^{-4} / P$$

→ e.g., thin (native) oxide layers form immediately (see next slide)
→ very difficult to keep clean metal surfaces in air

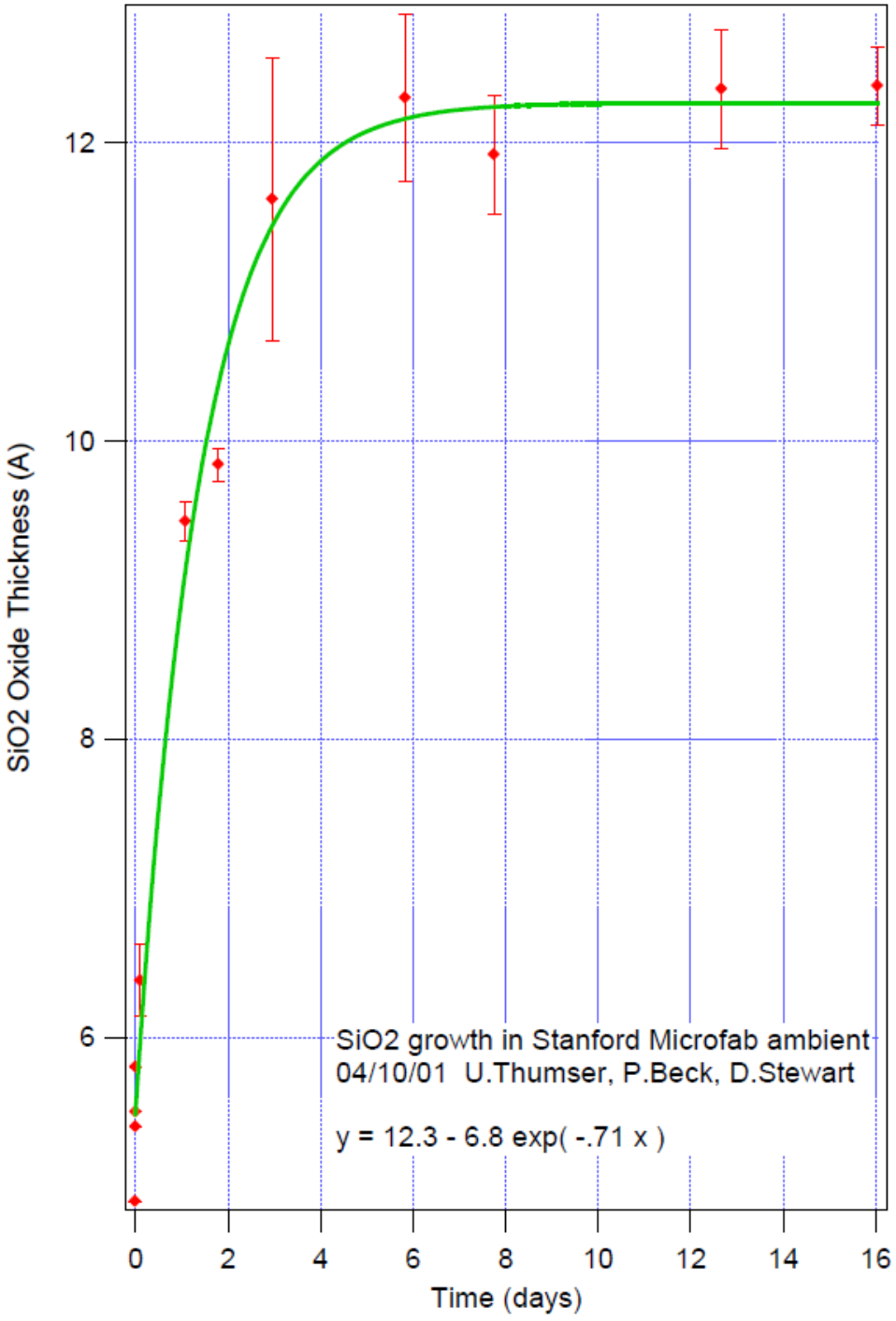
SiO2 Oxide Thickness (A)
12
10
8
6
0
2
4
6
8
10
12
14
16
Time (days)
SiO2 growth in Stanford Microfab ambient
04/10/01 U.Thumser, P.Beck, D.Stewart
y = 12.3 - 6.8 exp(-.71 x)

Commensurate monolayers, e.g., alkanethiols on Au

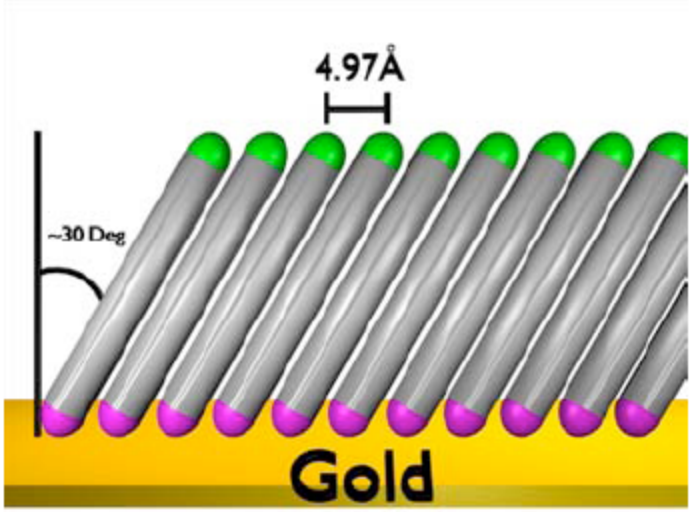

Figure 4a: The Au(111) lattice (yellow circles) is shown with a thiolate (purple circles) overlayer in a (√3 x √3)R30° arrangement. The distance between sulfur atoms is 4.99 Å.

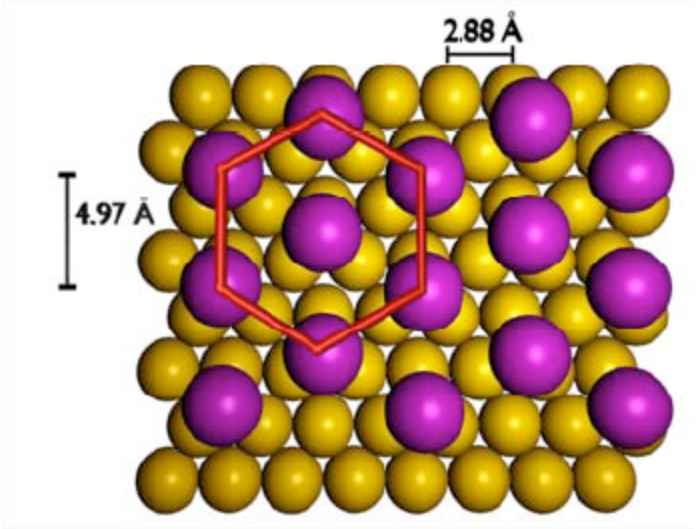

Figure 4b: A tightly packed alkanethiol monolayer is shown. In order to maximize the van der Waals forces between the alkane chains, the individual chains are tilted ~30° from the surface normal.

matching lattice constants

©2010 | A.J. Hart | 33

Multilayer SAMs

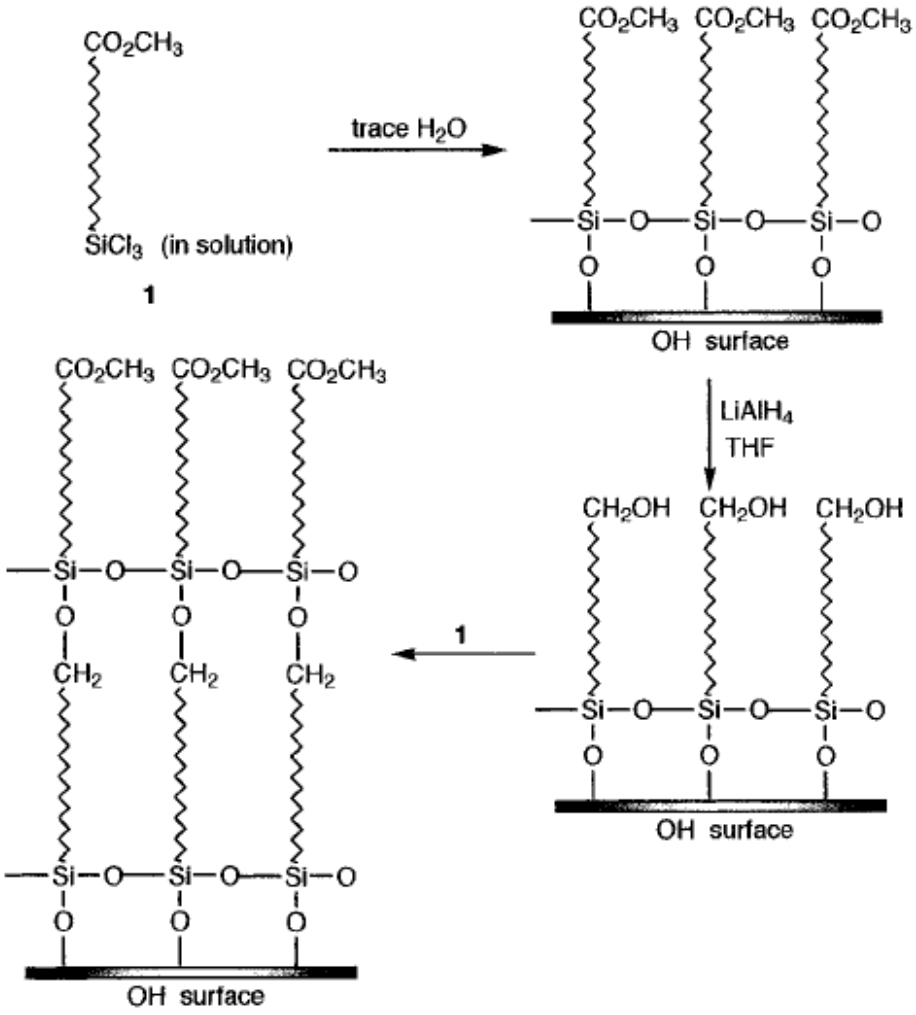

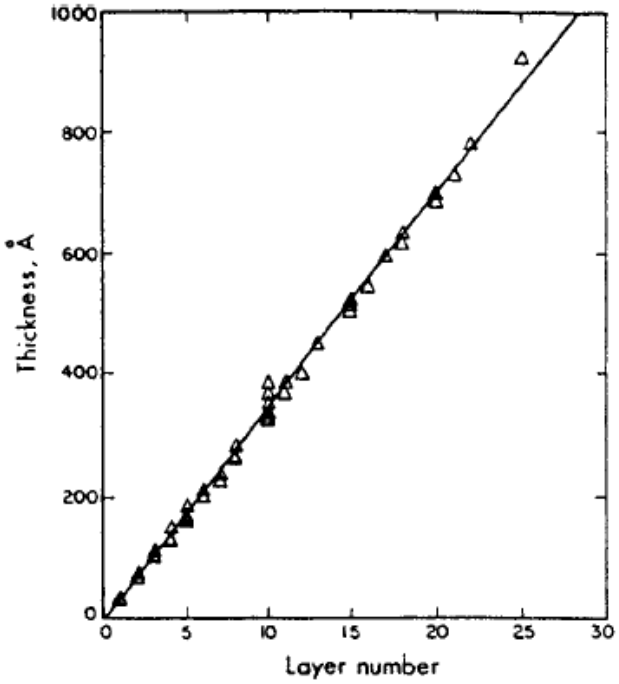

Figure 6. Film thickness vs layer number. (From Tillman et al., ref 61. Copyright 1988 American Chemical Society.)

Construction of multilayers requires that the mono-ıyer surface be modified to a hydroxylated one. uch surfaces can be prepared by a chemical reaction nd the conversion of a nonpolar terminal group to hydroxyl group. Examples of such reactions are ıe $LiAlH_4$ reduction of a surface ester group,[61] the hydroboration–oxidation of a terminal vinyl group,[23,59] and the conversion of a surface bromide using silver chemistry.[96] Once a subsequent monolayer is adsorbed on the "activated" monolayer, multilayer films may be built by repetition of this process (Figure 5).

Ulman, *Chem. Rev.* 96:1533, 1996.

What determines the uniformity and order of a SAM?

- Cleanliness and purity of the original surface
- Purity of the molecule and assembly solution
- Length and composition of the spacer chain
- Type of head group (size and properties), and the strength of its interaction with surface (reversibility)
- Amount of time the monolayer is allowed to assemble (e.g., "anneal")

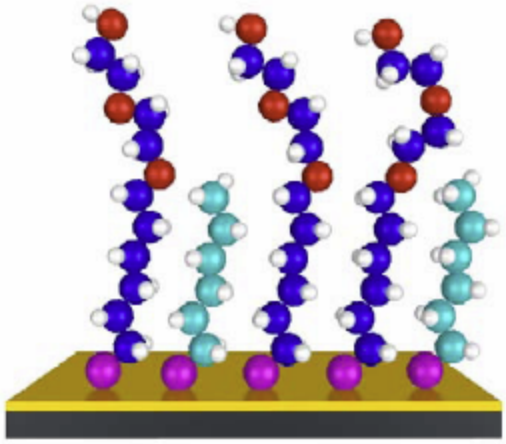

Figure 6. Illustration of a mixed SAM. This figure shows an illustration of a mixed SAM containing a short chain alkanethiol spacer mixed with an ethylene glycol terminated thiol. Mixtures of thiols can be used to generate unlimited possibilities in surface chemistry.

Mixed monolayers
(vs. domain separation)

Characterizing monolayers

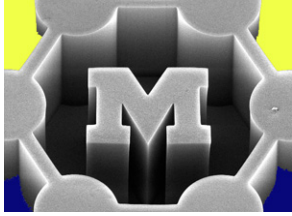

Method	Information
Contact angle measurement	Surface energy
Ellipsometry	Thickness
STM (scanning tunneling microscopy) and AFM (atomic force microscopy)	Imaging of monolayer texture, domain segregation, mechanical property and surface energy measurements
XPS (electron spectroscopy)	Chemical composition of surface; bonding configuration (hybridization)
FTIR (infrared spectroscopy)	Presence and order (orientation) of functional groups
SPR (surface plasmon resonance)	Direct monitoring of adsorption (kinetics)
Electron/X-ray diffraction	Geometric structure (packing, orientation)

STM images show domain separation in a mixed monolayers

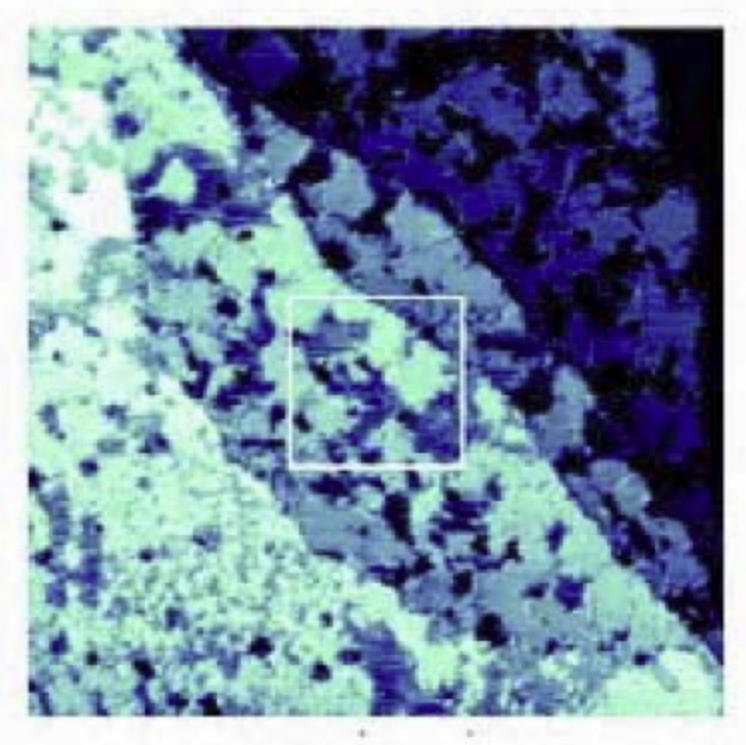

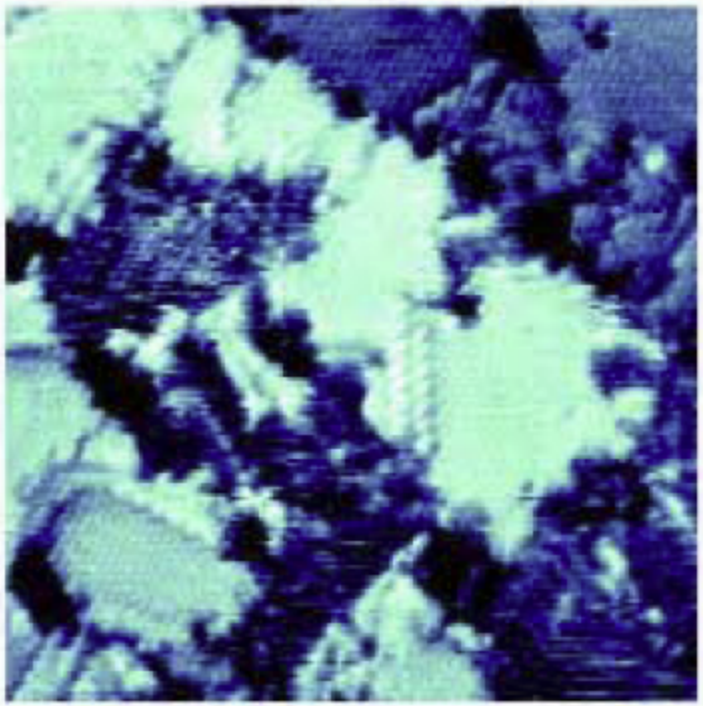

from F. Stellacci

Imaging SAMs on nanoparticles

- Using graphene as the TEM support

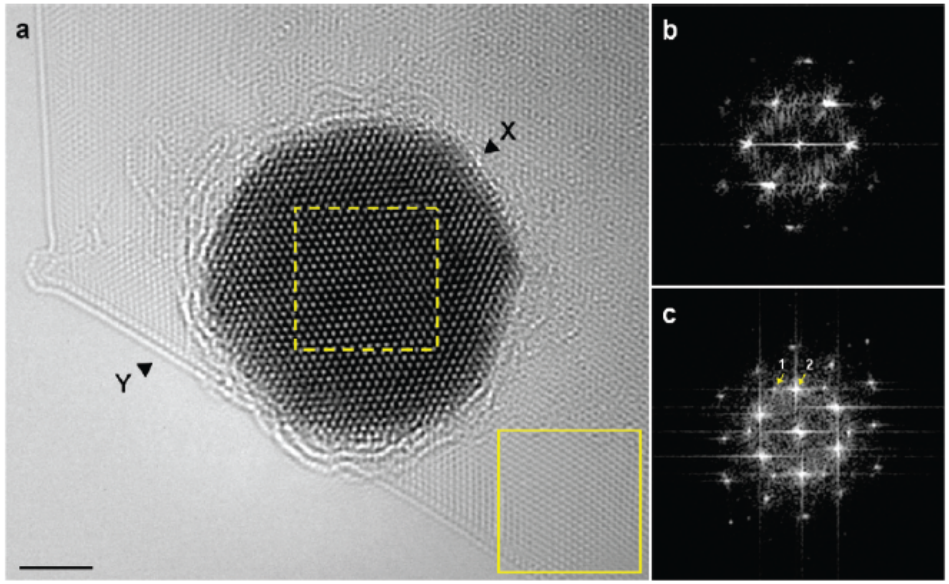

Citrate only (subtract Au and graphene)

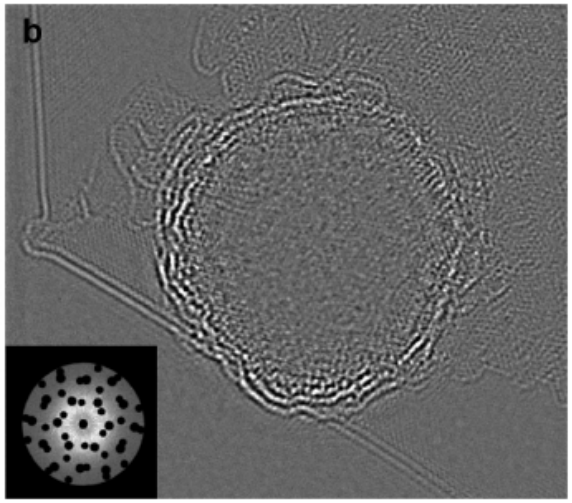

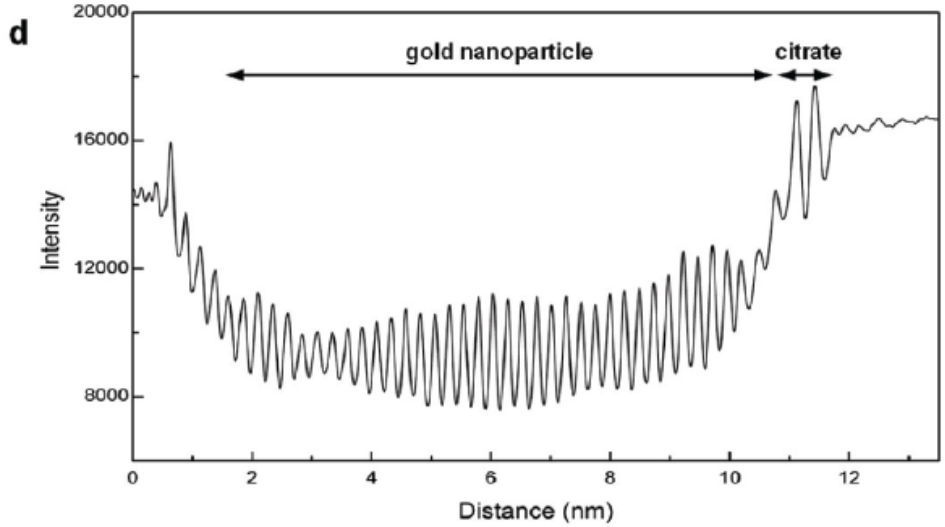

Lee et al., *Nano Letters* 9(9):3365-3369, 2009.

Self-stratified SAMs on Au nanoparticles

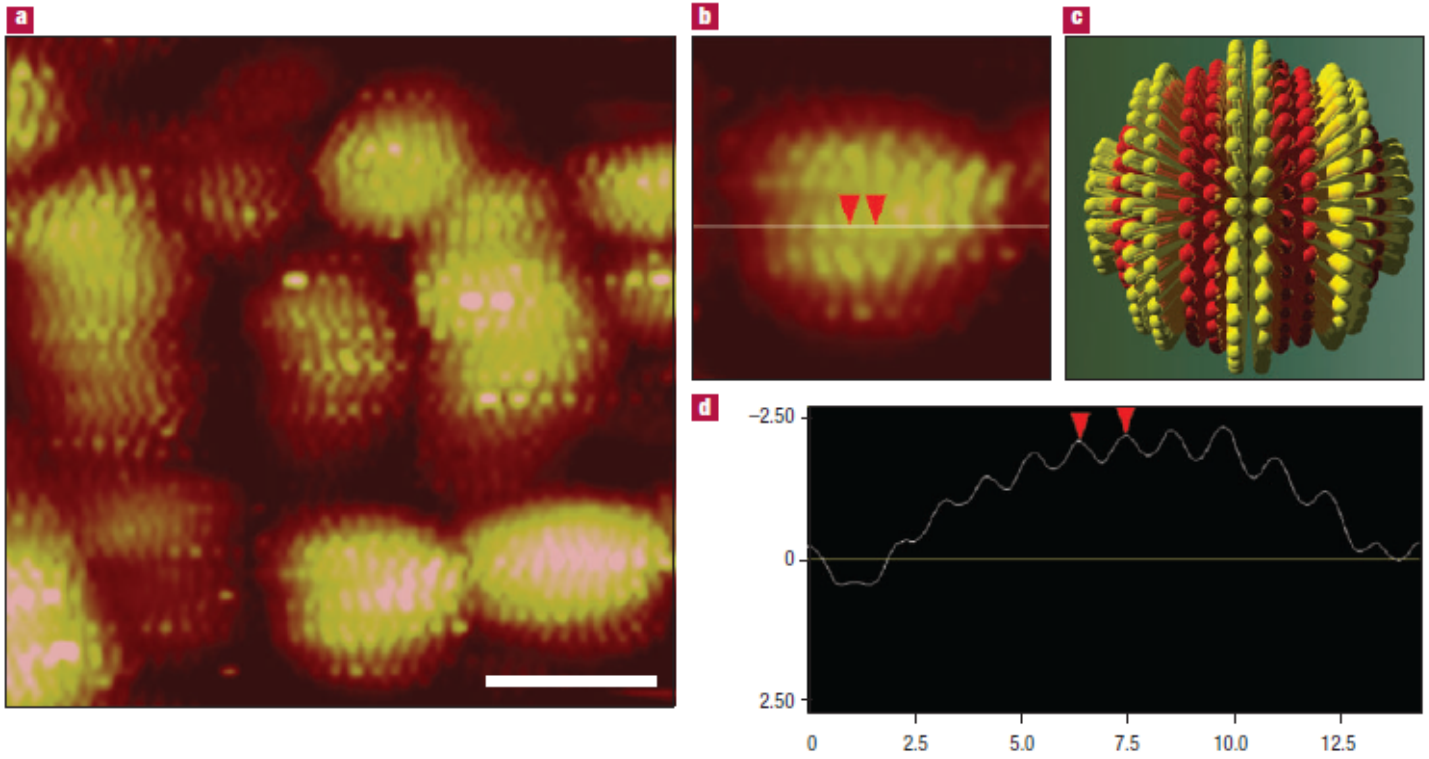

OT = octanethiol, CH_3-$(CH_2)_7$-SH; and
MPA = mercaptopropionic acid, HOOC-$(CH_2)_2$-SH,

Jackson, Myerson, Stellacci, *Nature Materials.* 3:1-7, 2004.

Domain organization determined by entropy and substrate curvature

Increasing chain length difference

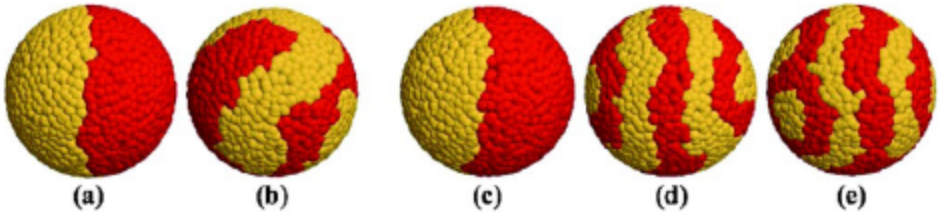

FIG. 3 (color online). Equilibrium structures obtained by mes-
oscale simulations of self-assembly of binary mixtures
factants with varying length difference or bulkiness differ
a sphere of radius 5σ. Dark (red) beads and light (yellow
represent head groups of the two species of surfactants (t
shown). (a) Length ratio 4:4, equal bulkiness. (b) Leng
6:6 with one surfactant (yellow heads) having a bulk
group. (c)–(e) Length ratios 4:6, 4:7 and 4:13, respe
with equal bulkiness.

- Chain length difference = chains want more room to maximize entropy
- Smaller particle = more room due to curvature

Increasing particle diameter

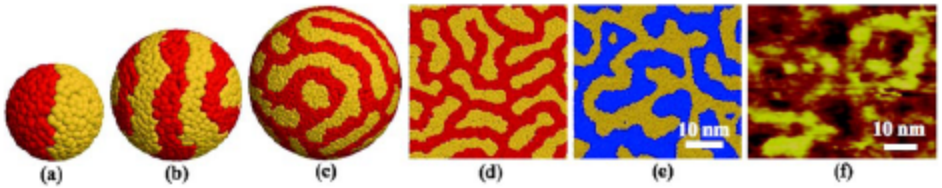

FIG. 4 (color online). (a)–(d) Equilibrium structures obtained by mesoscale simulations of self-assembly of a binary mixture of surfactants of length ratio 4:7 on surfaces with varying degrees of curvature. Dark (red) beads and light (yellow) beads represent head groups of shorter and longer surfactants, respectively (tails not shown). Sphere radius: (a) 3σ, (b) 5σ, (c) 10σ, (d) infinite. Sphere radii not drawn to scale. (e) Atomistic simulation of C4:C6 (both having -CH_3 tail end-group) mixed monolayer showing stripelike domains. Dark (blue) and light (yellow) beads are the head groups of the short and long surfactant, respectively. (f) STM height images of C4:C6 mixed monolayer showing stripelike morphology with a domain width of 5 nm.

Singh et al., *Phys. Rev Lett.* 99:226106, 2007.

Interfacial toughening using a monolayer

Interconnect structure
tested in 4-point bending

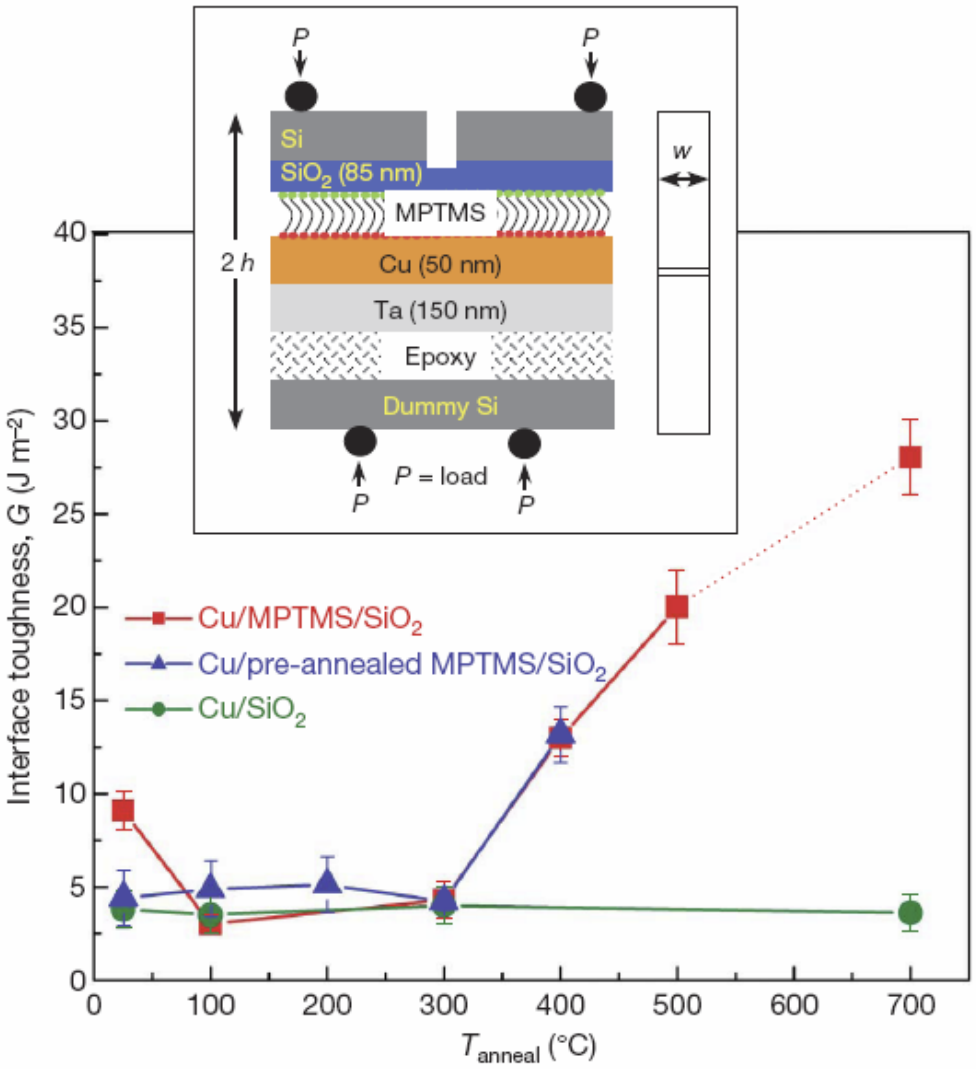

Quick calculation based on bond breakage confirms measured result

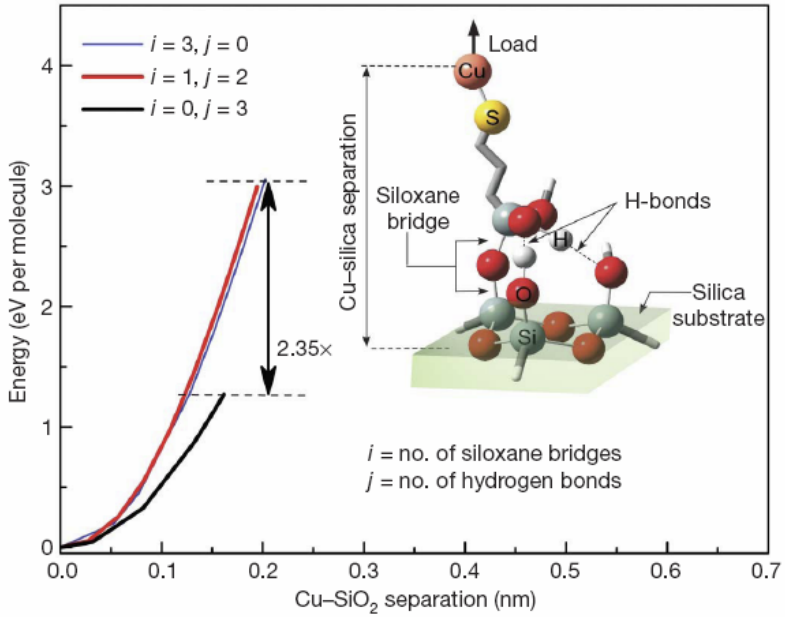

Figure 4 | Calculated system energy as a function of molecular stretching for different combinations of siloxane and hydrogen bonds at the MPTMS/SiO_2 interface. System energy was determined by first-principles density functional theory calculations. Inset, schematic depiction of an MPTMS molecule bonded to the silica underlayer by one siloxane bridge ($i = 1$, 33% irreversible dehydration) and two hydrogen bonds ($j = 2$). The arrow indicates the direction of stretching. The graph shows system energy plotted as a function of Cu overlayer/SiO_2 underlayer separation for three different interface bonding chemistries; each curve is plotted up to the fracture point.

Gandhi et al., *Nature* 447:299 2007.

XPS reveals Cu-S still bonded post-fracture

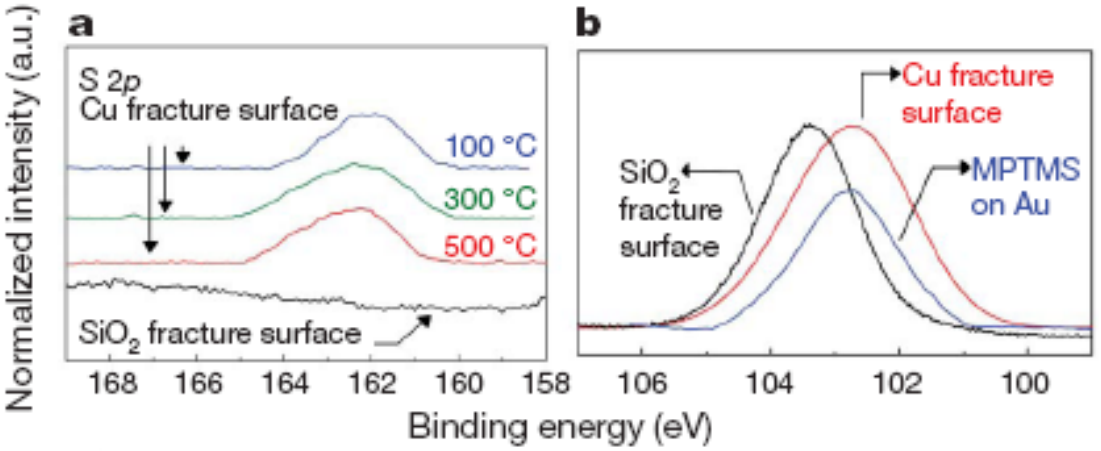

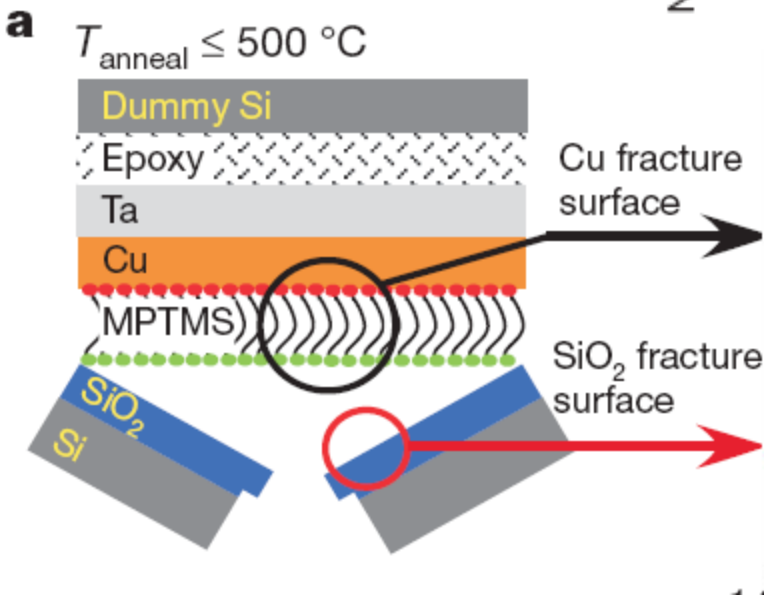

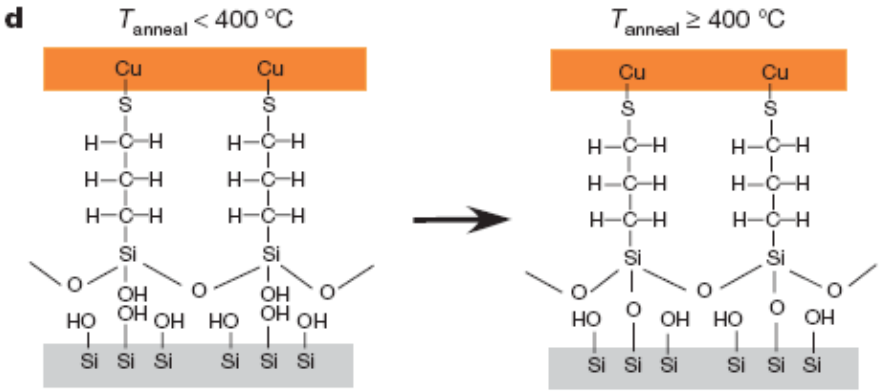

Figure 3 | High-resolution core-level spectra from fracture surfaces, and a schematic illustration of the primary toughening mechanism. **a**, S 2*p* bands from Cu fracture surfaces of samples for $T_{anneal} \leq 500\ ^{\circ}C$, shown with a reference spectrum from the silica fracture surface. **b**, Si 2*p* bands from Cu and silica fracture surfaces, respectively, shown with a reference spectrum from an MPTMS MNL on Au. **c**, S 2*p* intensity, normalized to the Cu 2*p* peak, plotted as a function of T_{anneal}. Data points, mean from four data sets; error bars, ±s.d. **d**, Schematic illustration of the temperature-assisted interfacial toughening mechanism. See text for details.

Annealing creates Si-O bonds (strong)
Cu layer prevents detachment

Gandhi et al., *Nature* 447:299 2007.

Langmuir-Blodgett method

Organize a monolayer on a liquid surface and draw a substrate vertically through the interface

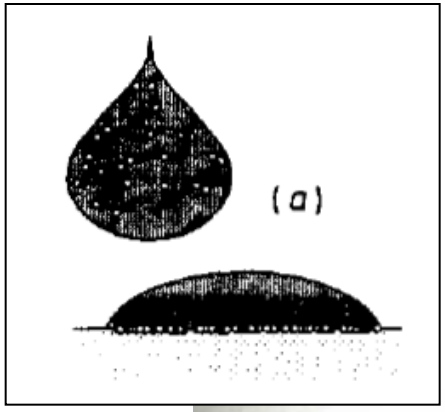

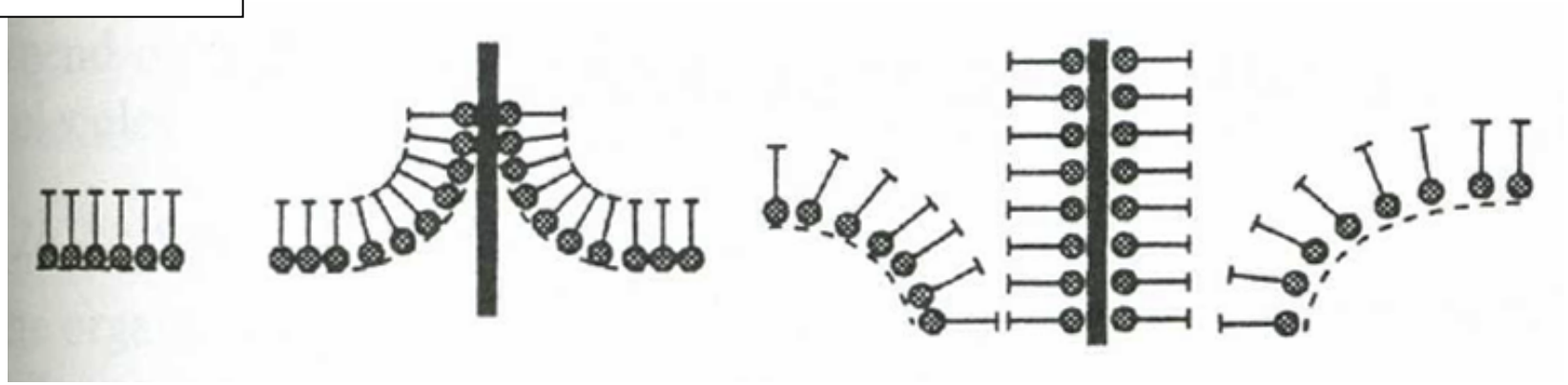

Developed at GE research laboratories, c.1915-1935

Irving Langmuir, Katharine Blodgett

Hiemenz and Rajagopalan.

Architectures of LB films

(for water surfaces)

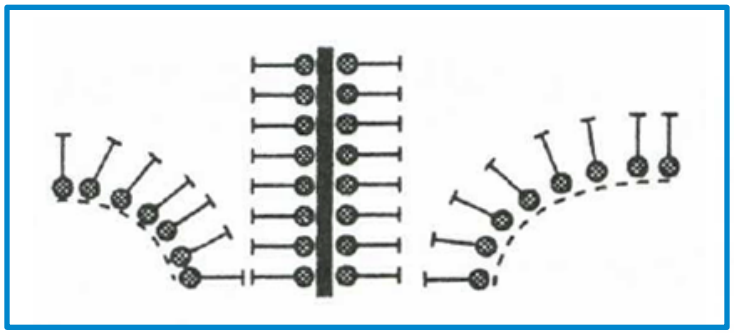

Hydrophobic substrate

immerse-immerse

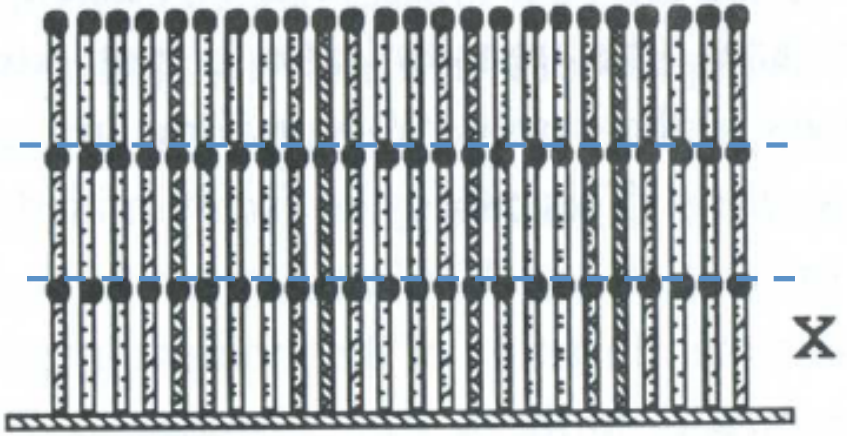

Hydrophilic substrate

withdraw-immerse

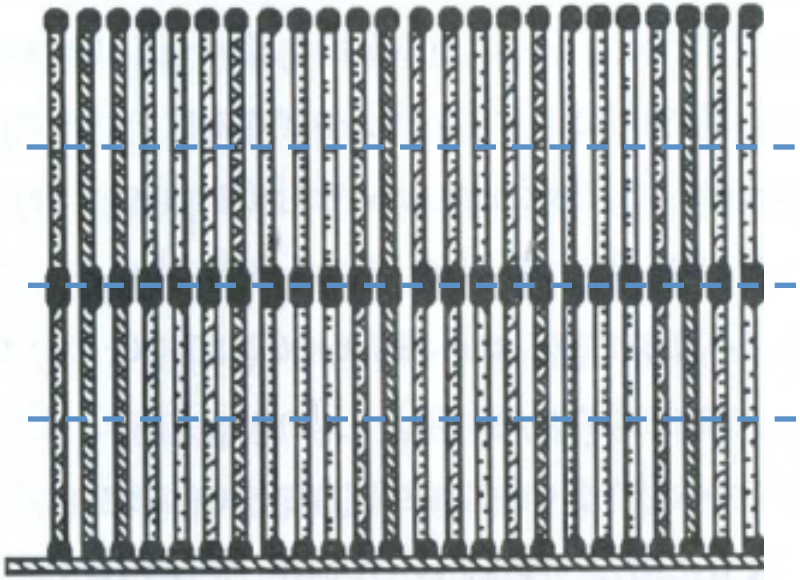

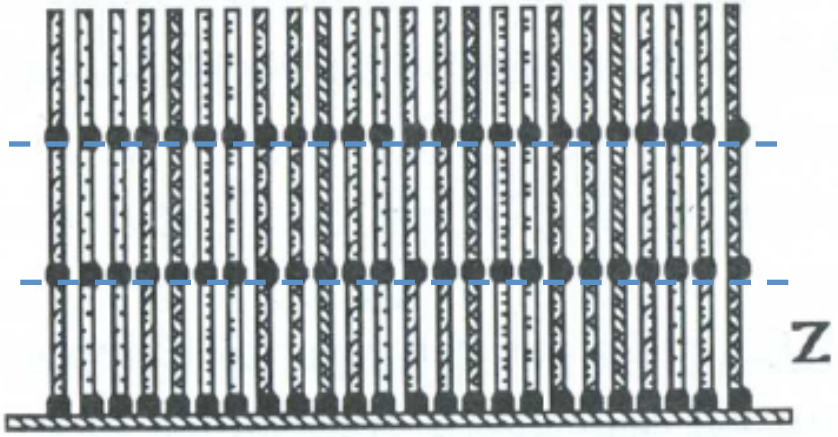

withdraw-withdraw

Langmuir-Blodgett trough – controlled deposition

Electrobalance senses surface pressure (tension) by moving barrier as deposition substrate is drawn through the surface

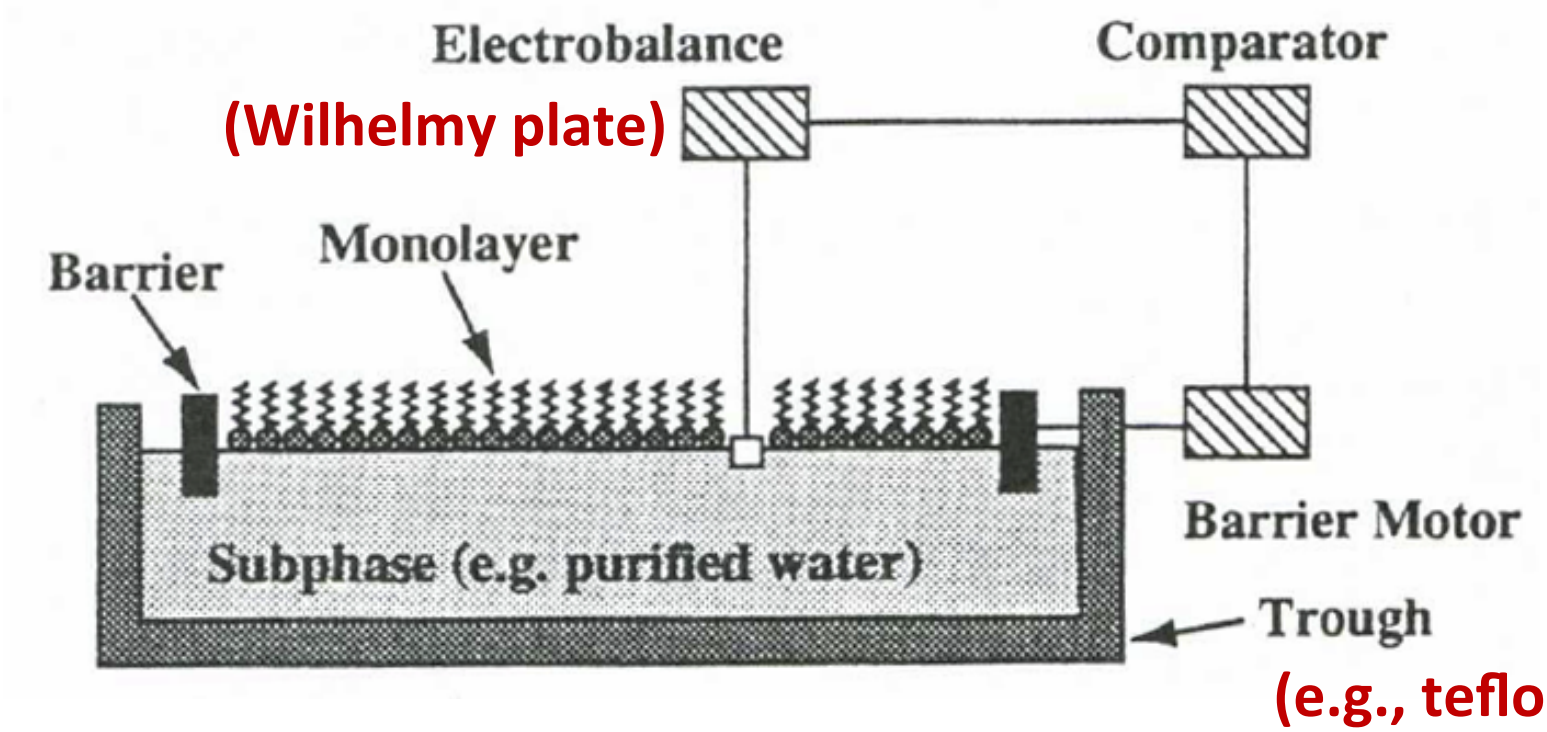

Hiemenz and Rajagopalan.

The pioneer: Agnes Pockels (1891)

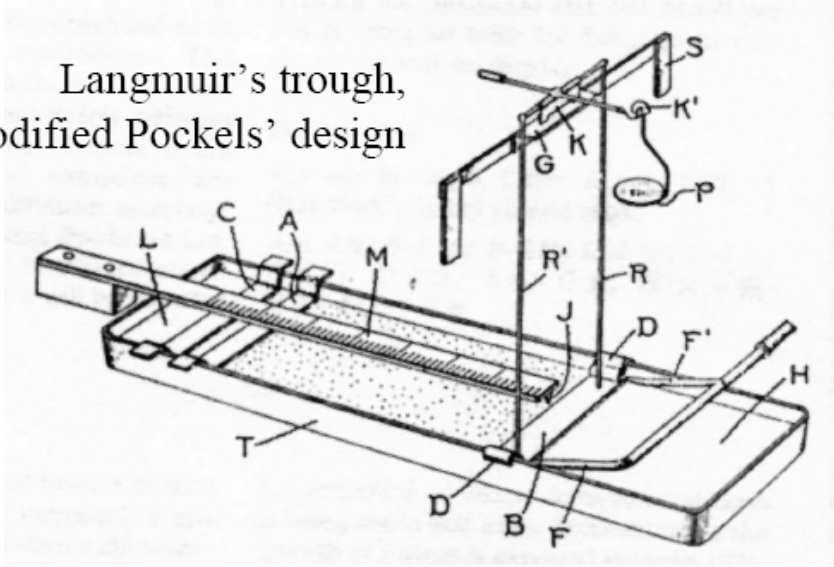

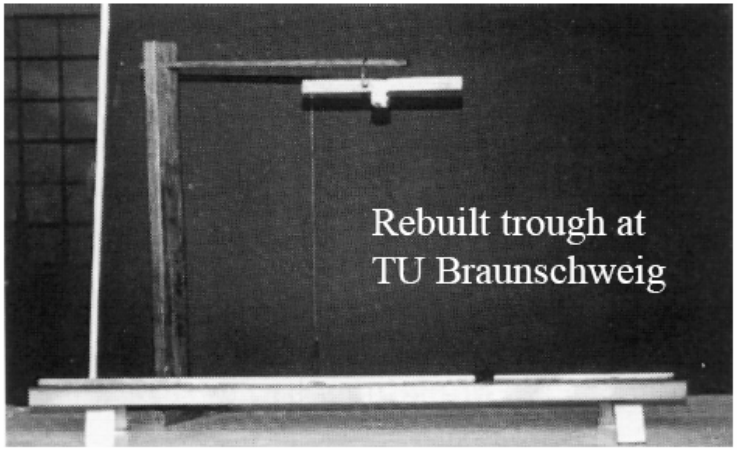

- "Rectangular tin trough, 70 cm long, 5 cm wide and 2 cm high filled with water to the brim and a strip of tin about 1.5 cm wide laid across it perpendicular to its length, so that the underside of the strip is in contact with the water."
- Vary of surface area by altering the strip position.
- Surface tension measured with an apothecary's balance → weight needed to lift a 6 mm diameter disk (i.e., a button) from the water.

Pockels, *Nature* 43:437, 1891.
http://www.aps.org/programs/women/workshops/upload/helm.pdf

Modern lab-scale LB trough

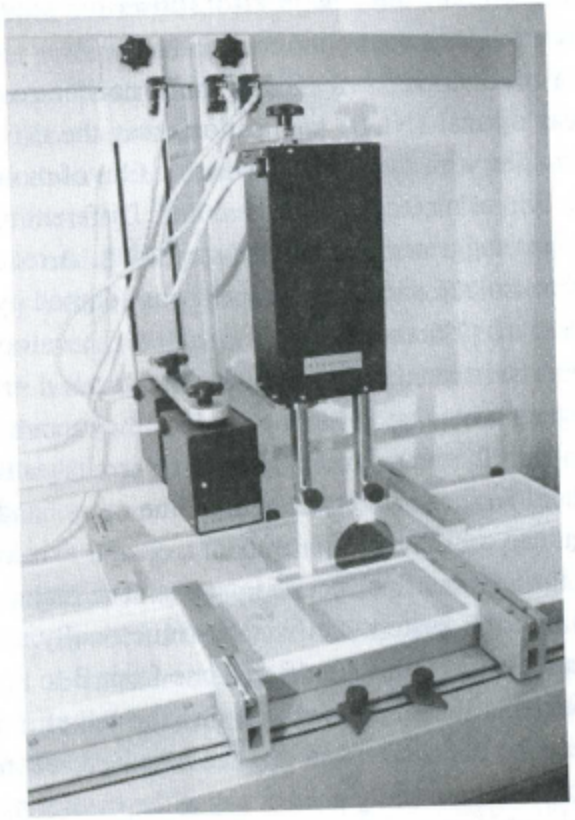

Figure 2.2. The KSV 5000 trough.

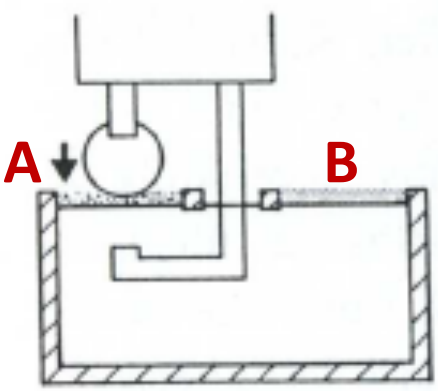

Step 1

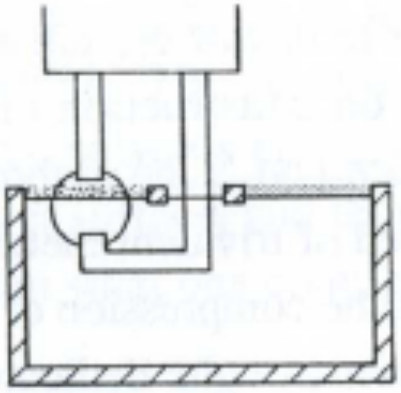

Step 2

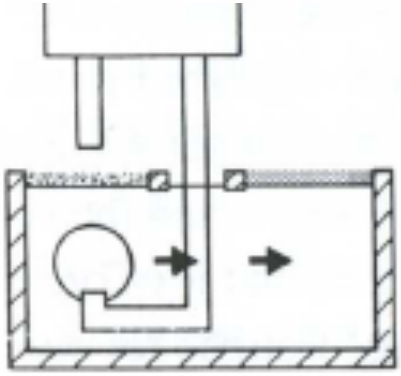

Step 3

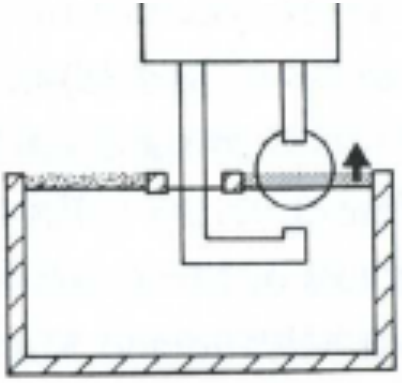

Step 4

Ulman.

Molecular compatibility

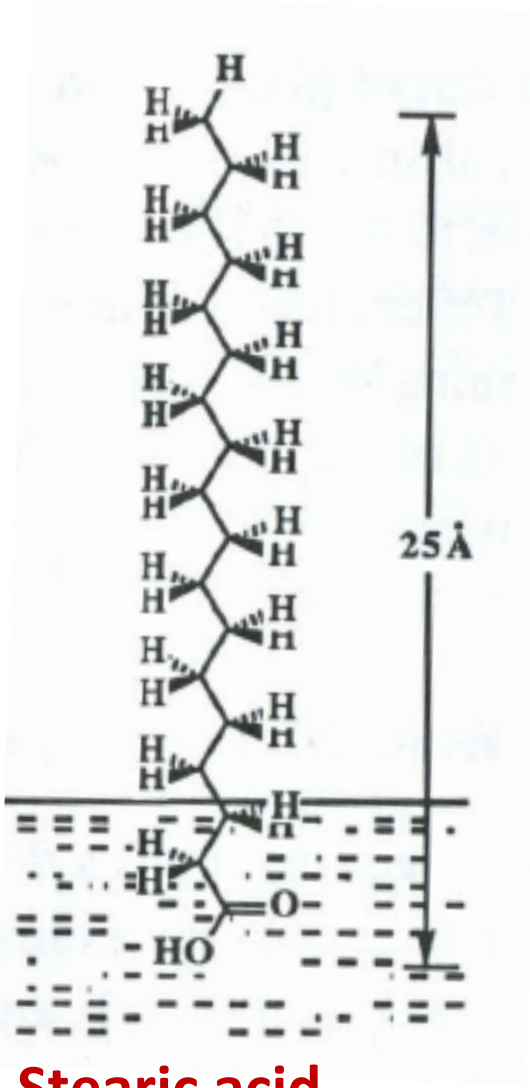

Table 2.1. The effect of different functional groups on film formation of C_{16}-compounds (Adapted from Adam [118].)

Very Weak (*no film*)	Weak (*unstable film*)	Strong (*stable film with C_{16} chain*)	Very Strong (C_{16} *compounds dissolve*)
Hydrocarbon	$-CH_2OCH_3$	$-CH_2OH$	$-SO_3^-$
$-CH_2I$	$-C_6H_4OCH_3$	$-COOH$	$-OSO_3^-$
$-CH_2Br$	$-COOCH_3$	$-CN$	$-C_6H_4SO_4^-$
$-CH_2Cl$		$-CONH_2$	$-NR_4^+$
$-NO_2$		$-CH{=}NOH$	
		$-C_6H_4OH$	
		$-CH_2COCH_3$	
		$-NHCONH_2$	
		$-NHCOCH_3$	

(e.g., form micelles)

Stearic acid

Hydrophilic end submerges part of chain

Ulman.

Table 3.1. Semiconductor Surface Preparation for LB Film Deposition

Semiconductor	Surface treatment	LB film material	References
Si single crystal	HF followed by refluxing in CCl_3CH_3 with small addition of $Si(CH_3)_2Cl_2$ *or* 5 min in $[(CH_3)_3\ Si]_2\ NH$	ω-Tricosenoic acid α-Octadecylacrylic acid	169—171
α-Si:H thin film	2.5 min in 40% HF:40% NH_4F (1 : 5 ratio by volume) follwed by 10 min in chlorine water	Cadmium stearate	172
GaAs epitaxial layer	1 min in Br_2/methanol (1 : 2000 by volume), 5 min in conc HCl followed by methanol rinse	ω-Tricosenoic acid	173
GaP single crystal	3 min in $H_2SO_4 : H_2O_2 : H_2O$ (4 : 1 : 1 by volume) followed by 1 min $H_2O_2 : H_2O$ (1 : 20 by volume) containing 2 g NaOH per 100 ml of solution	Preformed polymers Cadmium stearate Chlorophyll	174–176
GaP epitaxial film	30 s in 3 g $K_3Fe(CN)_6$, 0.24 g KOH and 10 cm^3 H_2O at 80 °C	Cadmium stearate ω-Tricosenoic acid Phthalocyanine	177
InP single crystal	$H_2SO_4 : H_2O_2 : H_2O$ (4 : 1 : 1 by volume) followed by *either* a 20% solution of $Br_2/HBr/H_2O$ (1 : 17 : 35 by volume) *or* $HCl : H_2O_2 : H_2O$ (1 : 1 : 10 by volume)	Cadmium stearate	167
InSb, CdTe, CdS, ZnS (single crystals); ZnSe (epitaxial films)	Bromine in methanol (0.5–1% by volume)	Cadmium stearate Substituted anthracene derivative (for CdTe)	178–182

©2010 | A.J. Hart | 49

Floating monolayer as a "2D gas"

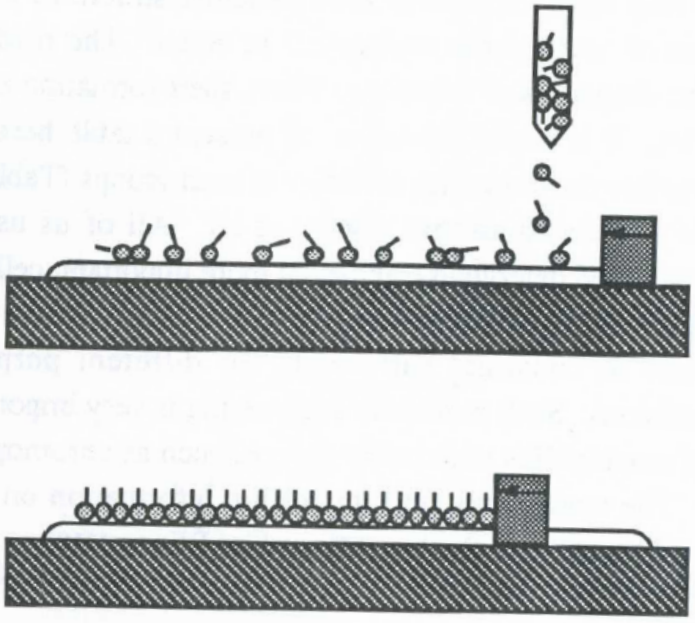

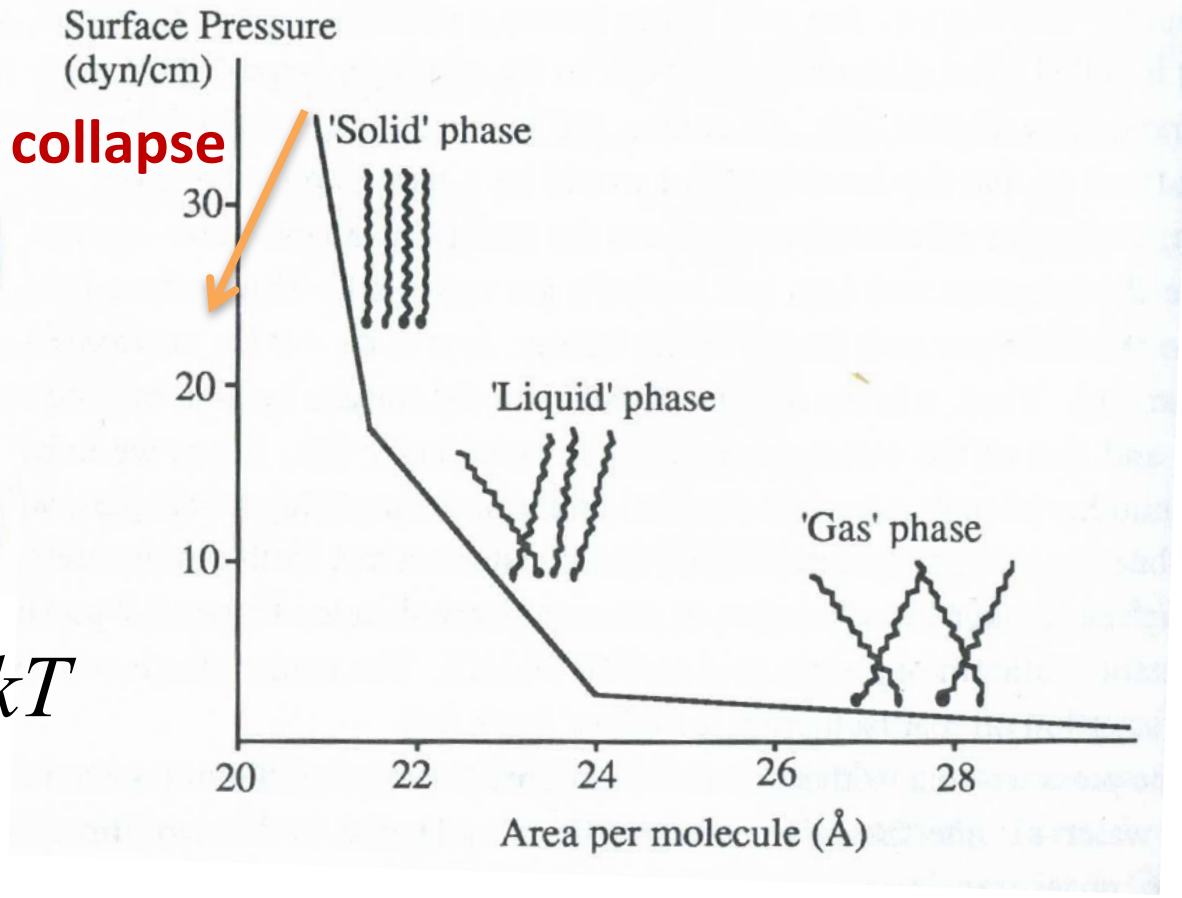

$$\pi A = kT$$

Surface tension x Area

Number of molecules per unit area known from initial droplet concentration

©2010 | A.J. Hart | 50

Process control windows

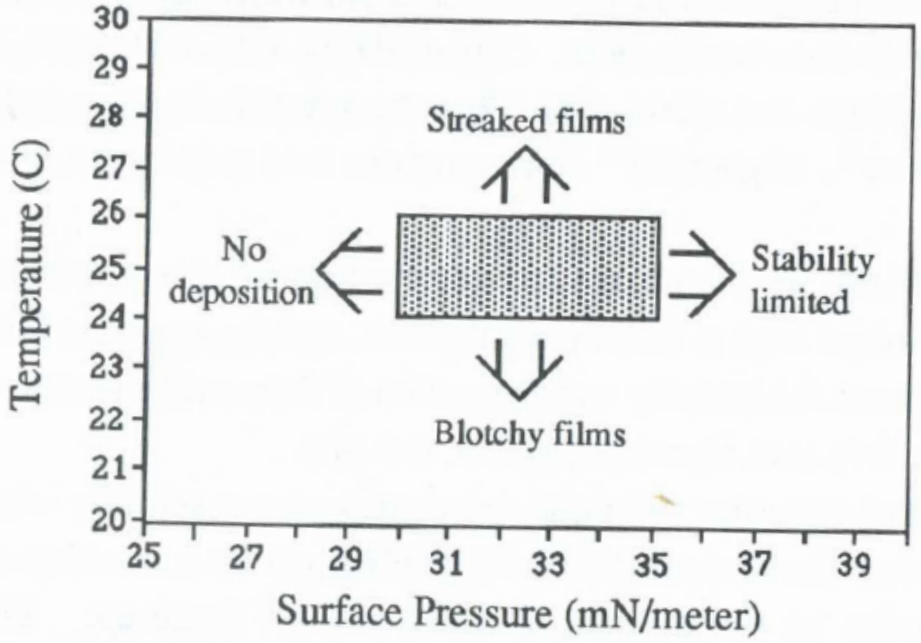

Figure 2.14. Processing window for brassidic acid monolayers. The parameters used were "aged" water or low concentration of $CdCl_2$, 0.5–1 mg/mL brassidic acid concentration, spreading area of 60 $Å^2$/molecule, dwell period of 10 mim, compression rate of 2 cm/min and dipping velocity of 1–3 mm/min. (Adopted from Biddle *et al.* [136], © 1985, Elsevier Science Publishers.)

- Longer chain (higher "viscosity") → lower maximum deposition speed

Ulman.

LB processing considerations

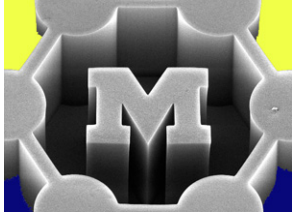

- Low vibration environment
- No atmospheric contaminants
  - clean air, laminar flow hood

- Clean subphase
  - e.g., deionized and filtered water
- Clean substrate
  - e.g., piranha-cleaned Si, which then grows native SiO_2
  - most often hydrophilic for deposition in retraction mode

- High-purity amphiphiles and solvents
- Wash bath using inorganic detergents

©2010 | A.J. Hart |

Continuous LB deposition

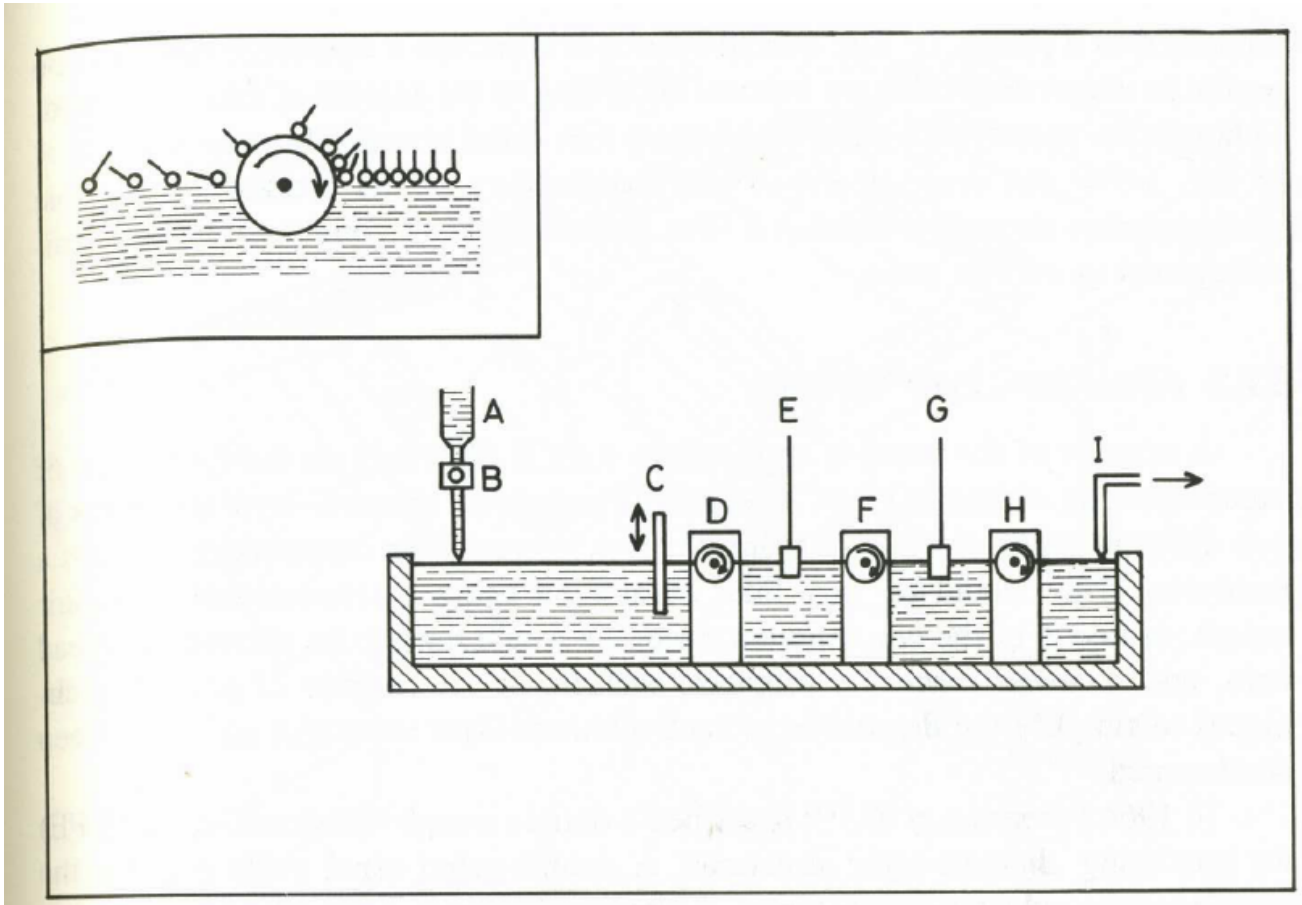

Figure 3.15. Trough for continuous deposition of monolayers (after Barraud and Vandevyver[92]). The inset shows a roller working in the "hydrophobic" mode to compress the monolayer.

Surface printing (Schaefer method)

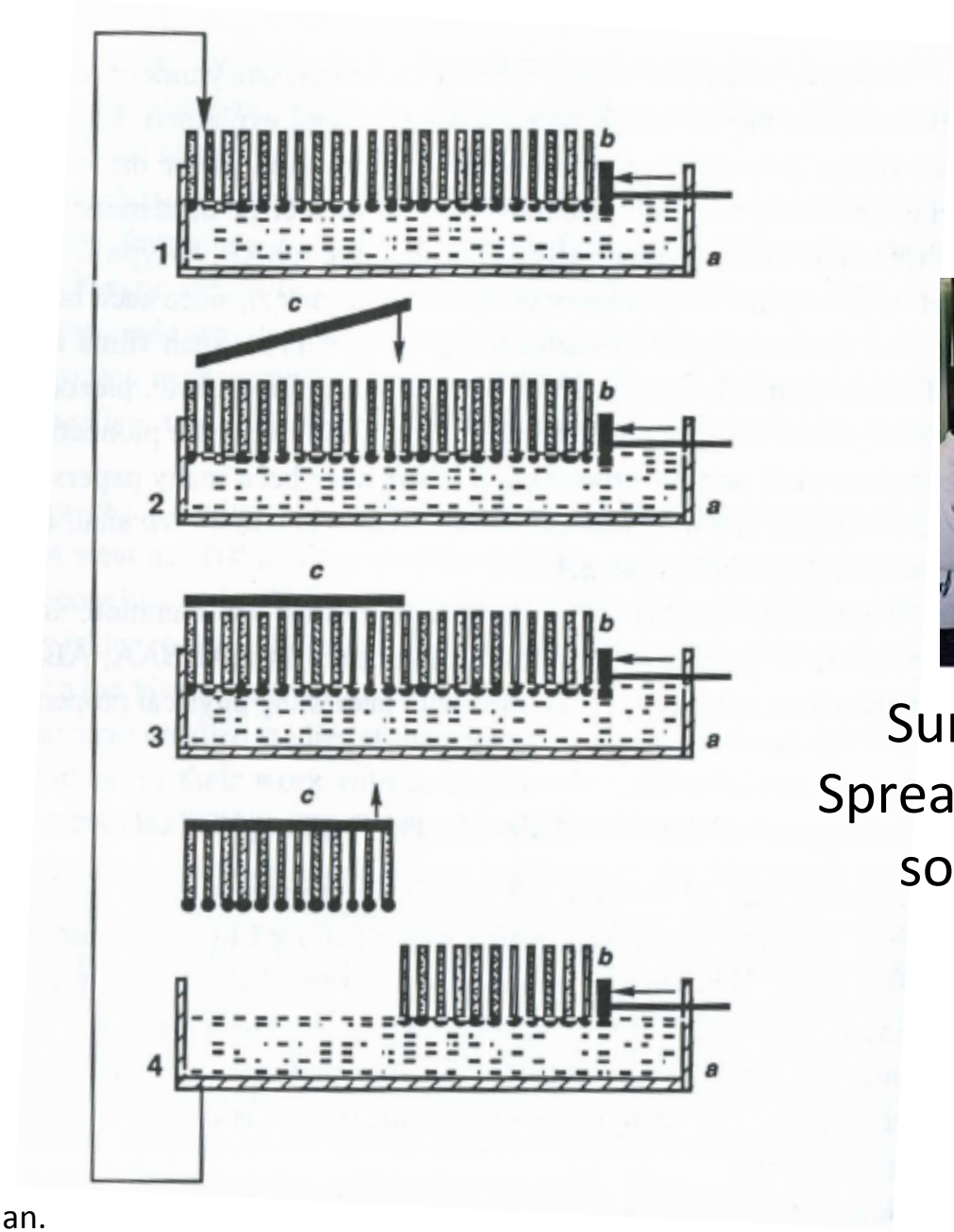

Suminagashi ("floating ink")
Spread carbon particles in protein solution on a water surface

http://www.suminagashi.com

Ulman.

LB of Ag nanowires (like logging)

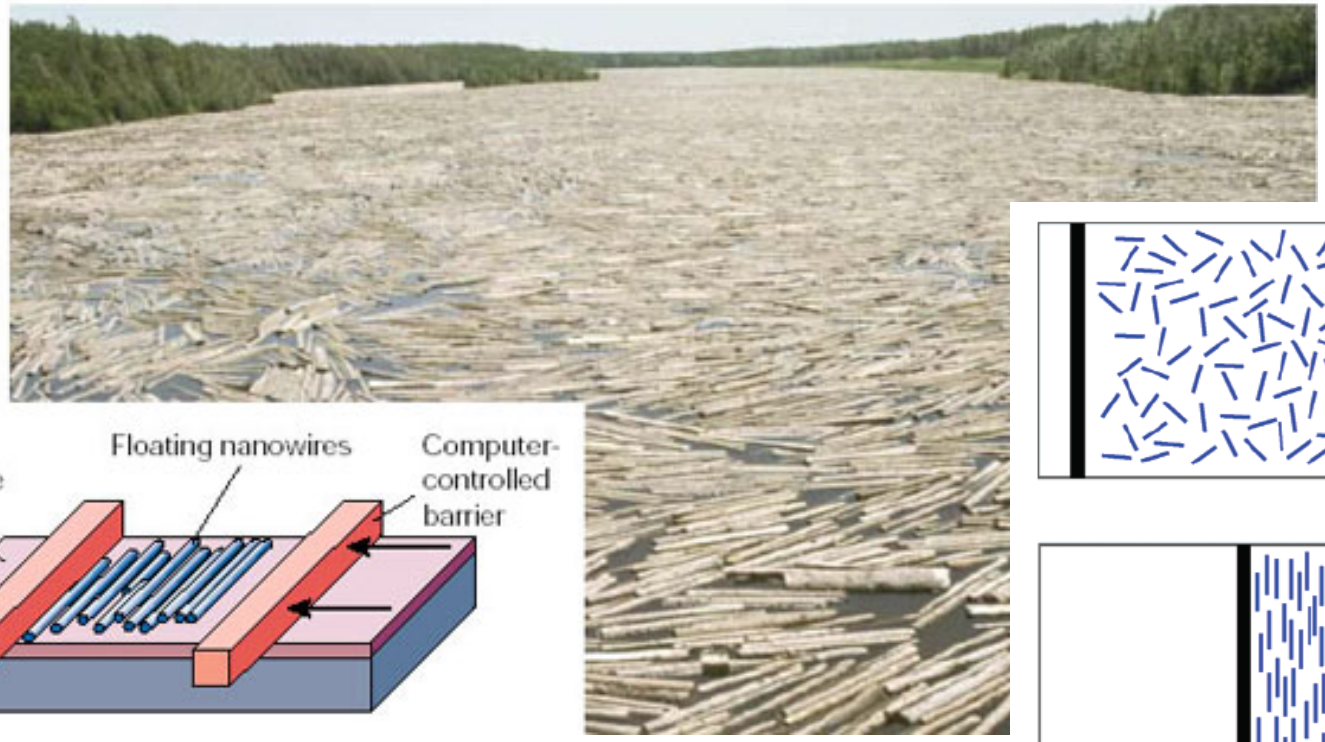

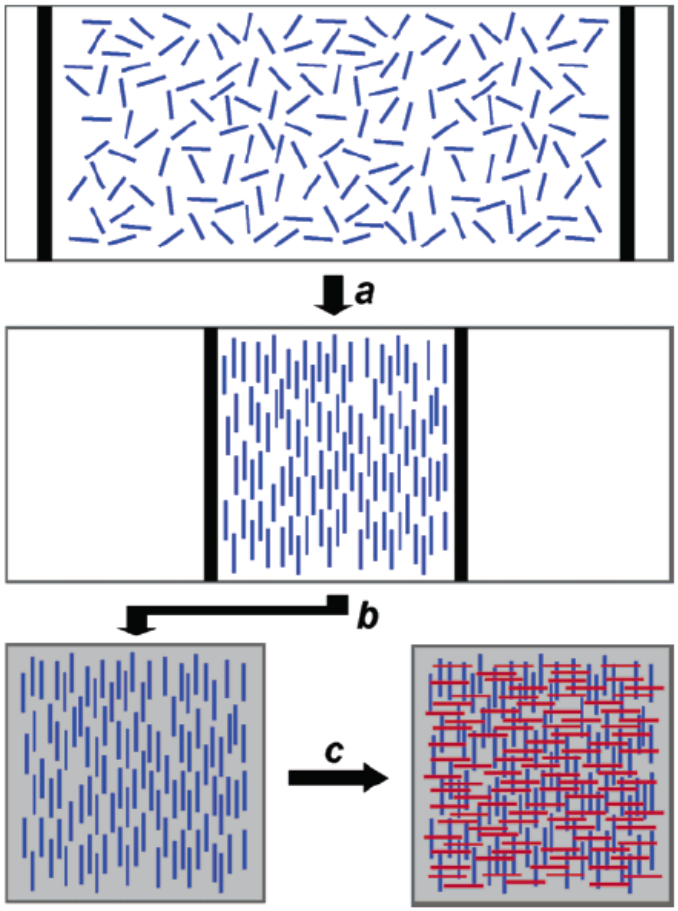

Tao et al., *Nano Lett.* 3(9):1229, 2003.
Whang et al., *Nano Lett.* 3(9):1255, 2003

Surface pressure increases as monolayer is compacted

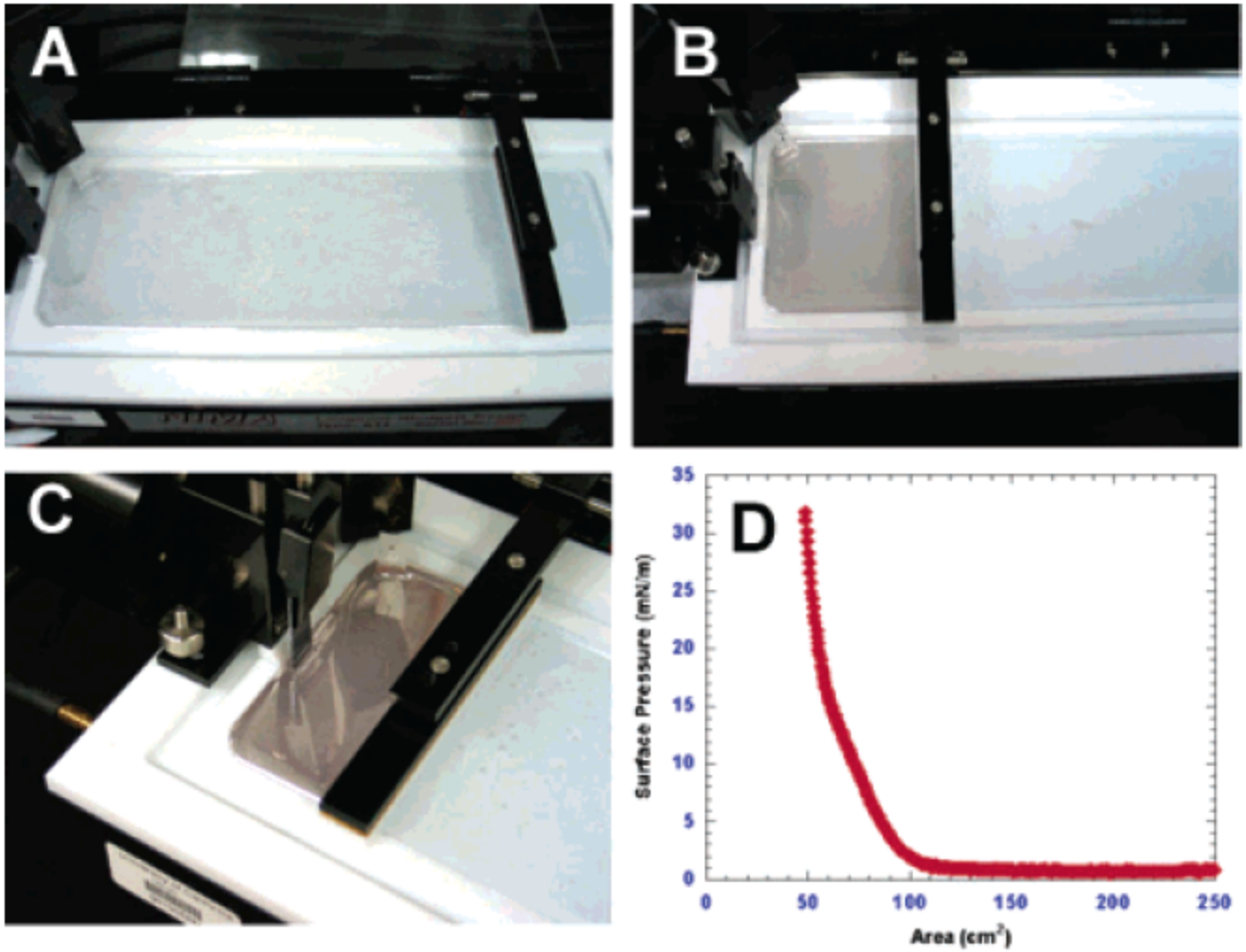

Tao et al., *Nano Lett.* 3(9):1229, 2003.

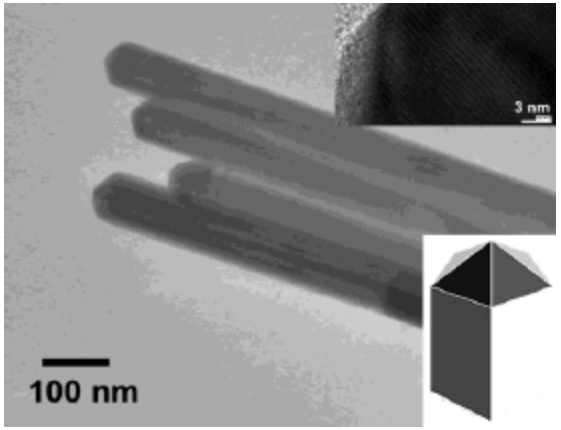

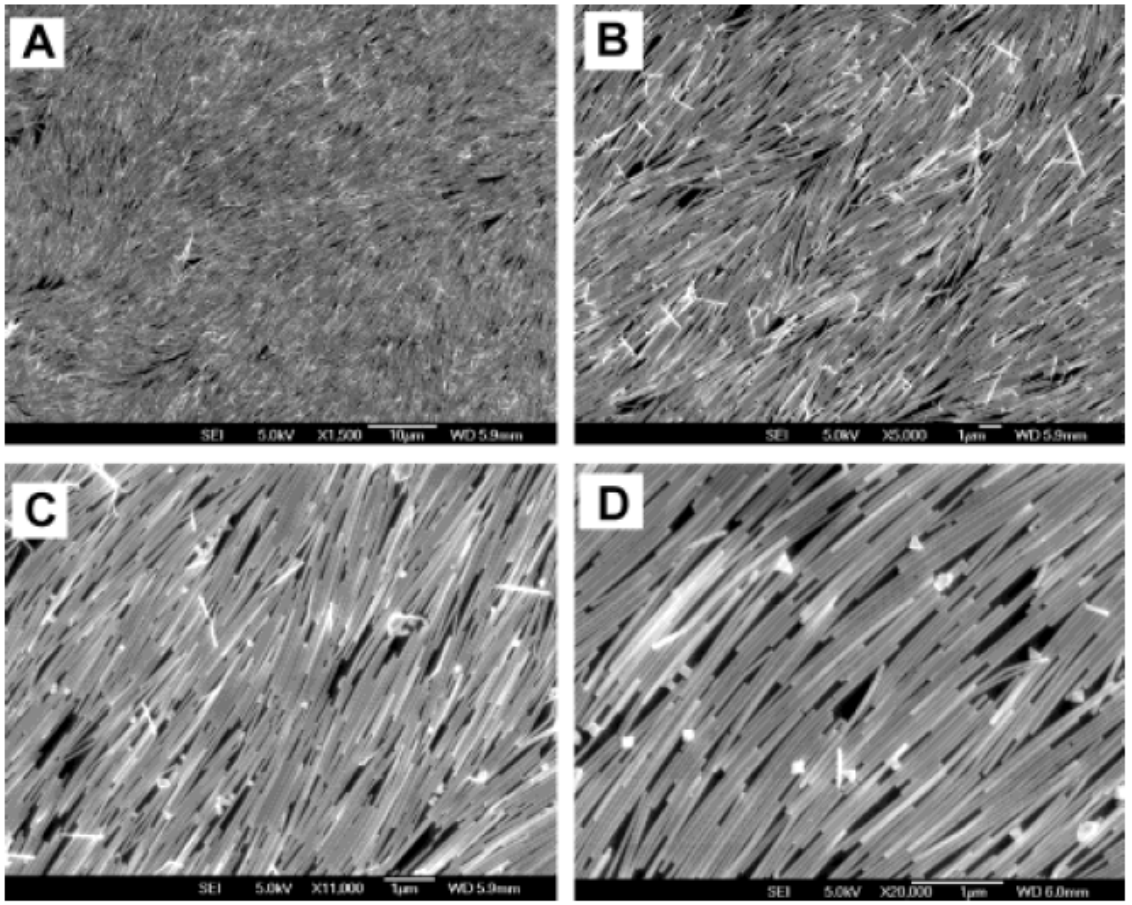

Figure 3. Scanning electron microscopy images (at different magnifications) of the silver nanowire monolayer deposited on a silicon wafer.

Tao et al., *Nano Lett.* 3(9):1229, 2003.

LB deposition of graphene (oxide) films

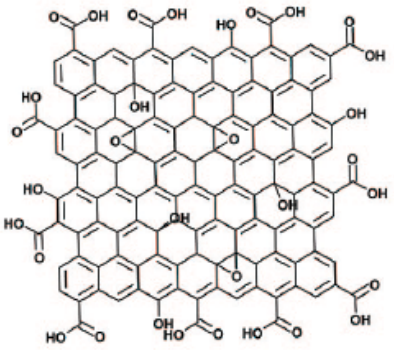

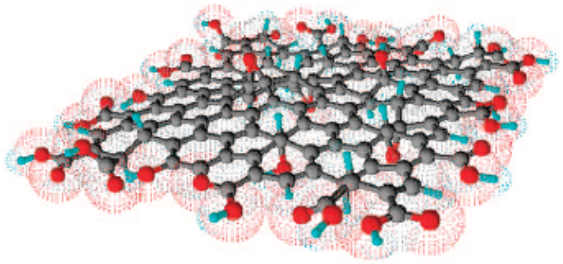

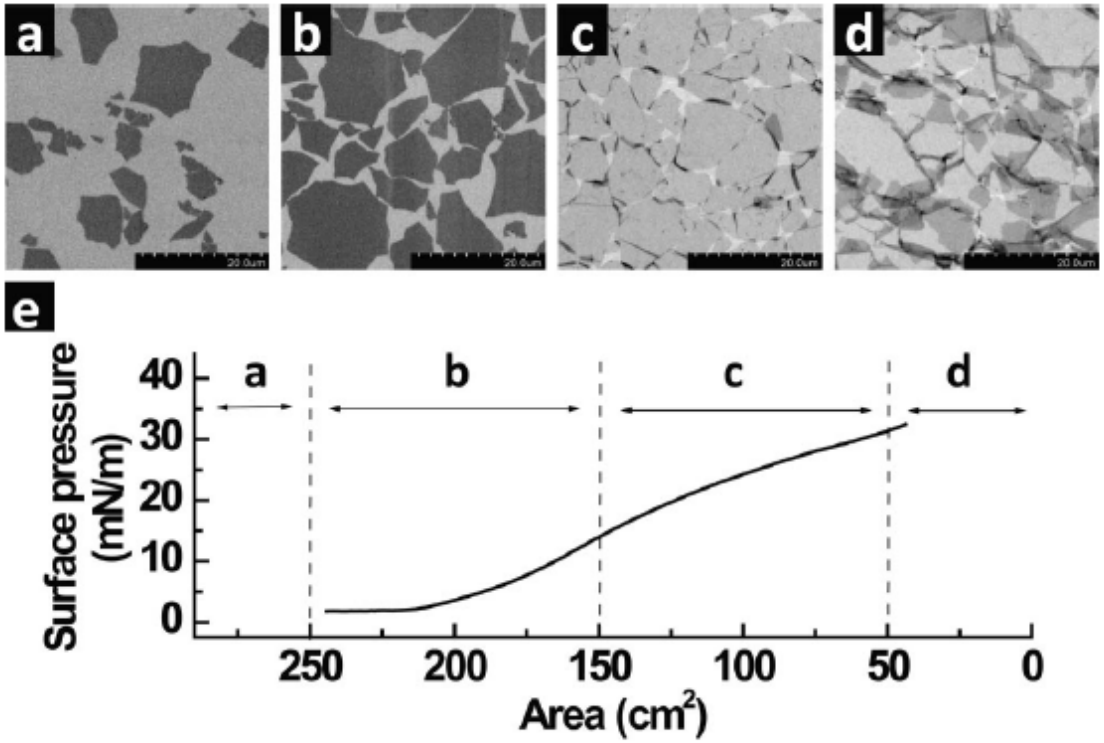

Figure 2. Langmuir−Blodgett assembly of graphite oxide single layers. (a−d) SEM images showing the collected graphite oxide monolayers on a silicon wafer at different regions of the isotherm. The packing density was continuously tuned: (a) dilute monolayer of isolated flat sheets, (b) monolayer of close-packed GO, (c) overpacked monolayer with sheets folded at interconnecting edges, and (d) over packed monolayer with folded and partially overlapped sheets interlocking with each other. (e) Isothermal surface pressure/area plot showing the corresponding regions a−d at which the monolayers were collected. Scale bars in a-d represent 20 μm.

Cote et al., JACS 131:1043-1049, 2009.

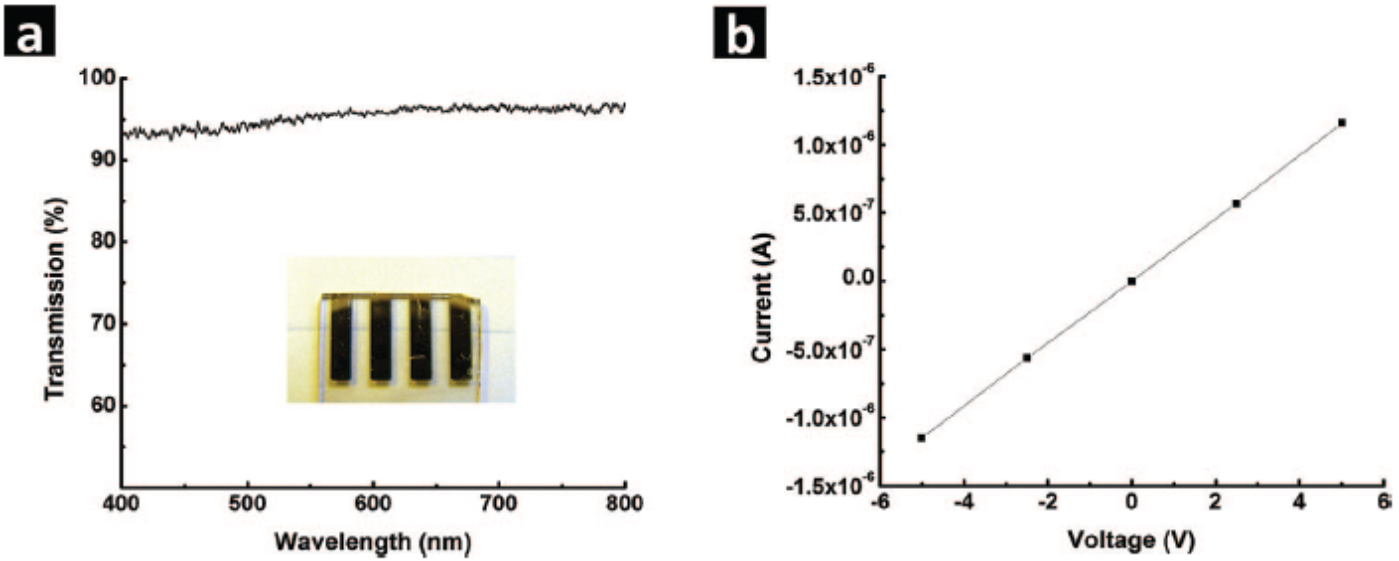

Figure 6. Transparent conducting thin film obtained by chemical reduction of an overpacked, interlocking GOSL monolayer such as those collected from region d of the isotherm plot in Figure 2. (a) Transmission spectrum of such a thin film deposited on a glass slide (inset), showing an average of 95.4% transmittance in the visible region. (b) Current−voltage plot of the same film obtained by four-point measurement.

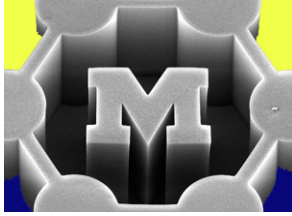

Extras

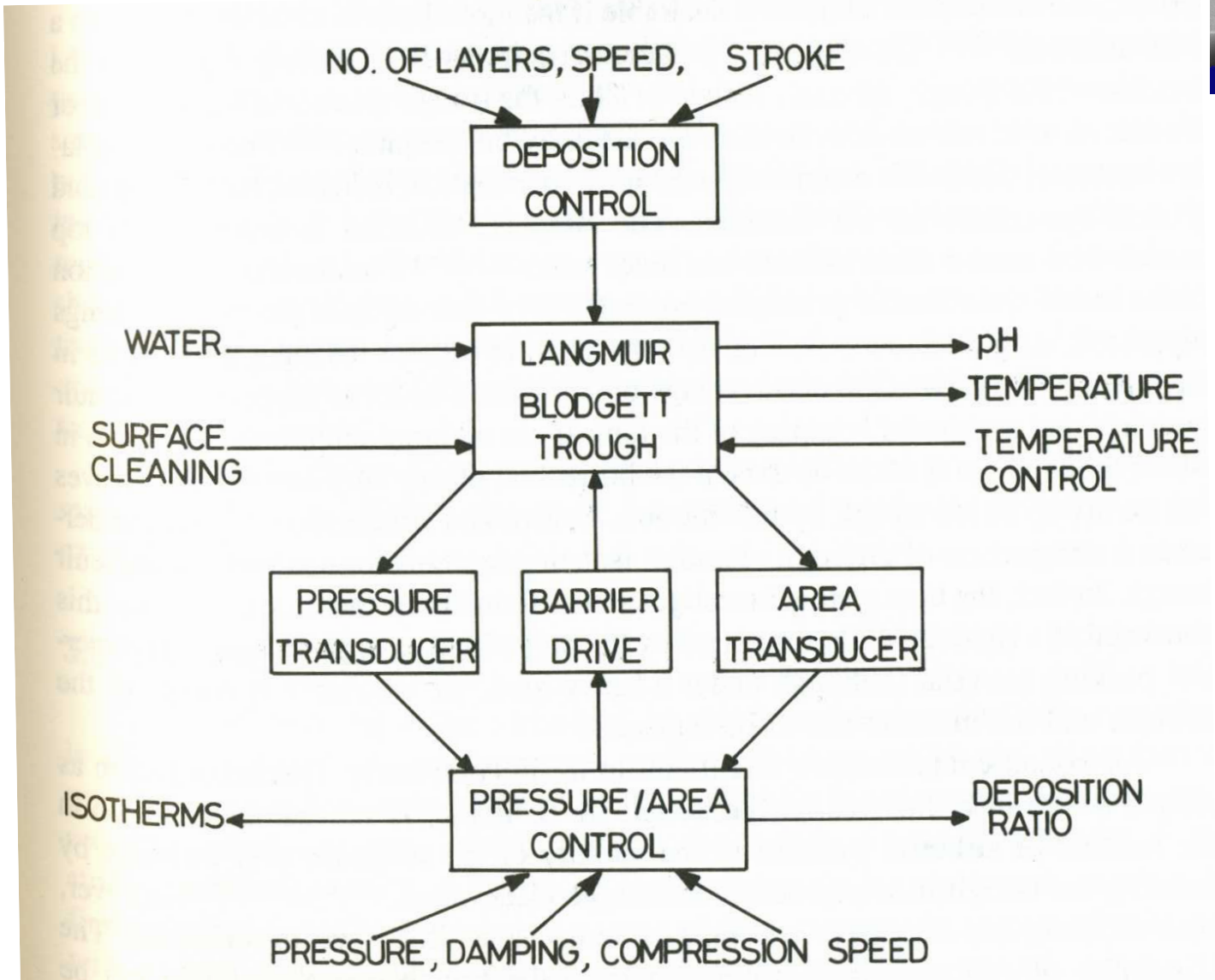

Figure 3.14. Block diagram showing LB trough services.

©2010 | A.J. Hart | 61

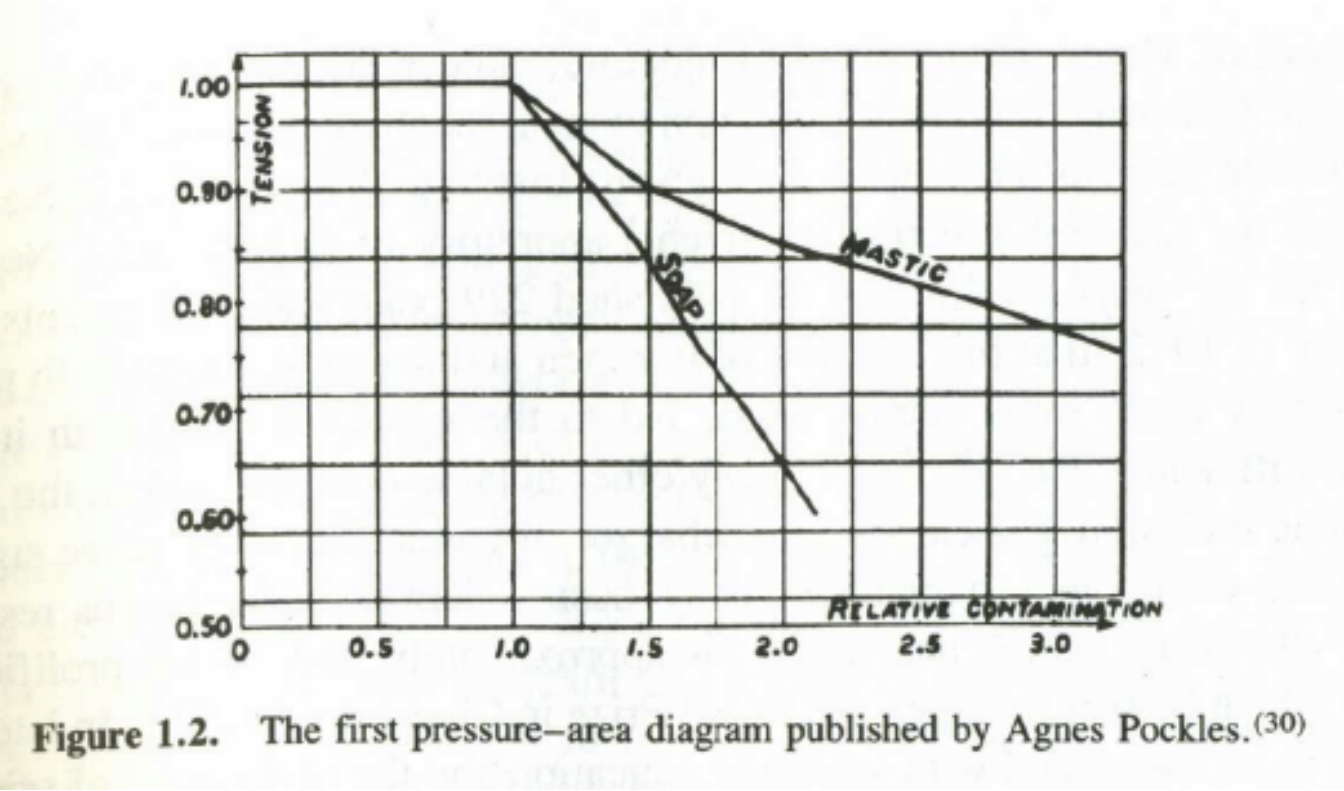

Figure 1.2. The first pressure–area diagram published by Agnes Pockles.[30]

"A water surface can exist in two states, a *normal condition* in which the surface tension remains constant if the surface size is changed, and an *anomalous condition,* where varying the surface size leads to a change in surface tension."

"The cleaner the surface, the more it can be compressed while the surface pressure remains at its maximum value."

Pockels, *Nature* 43:437, 1891.
http://www.aps.org/programs/women/workshops/upload/helm.pdf

Wilhelmy plate

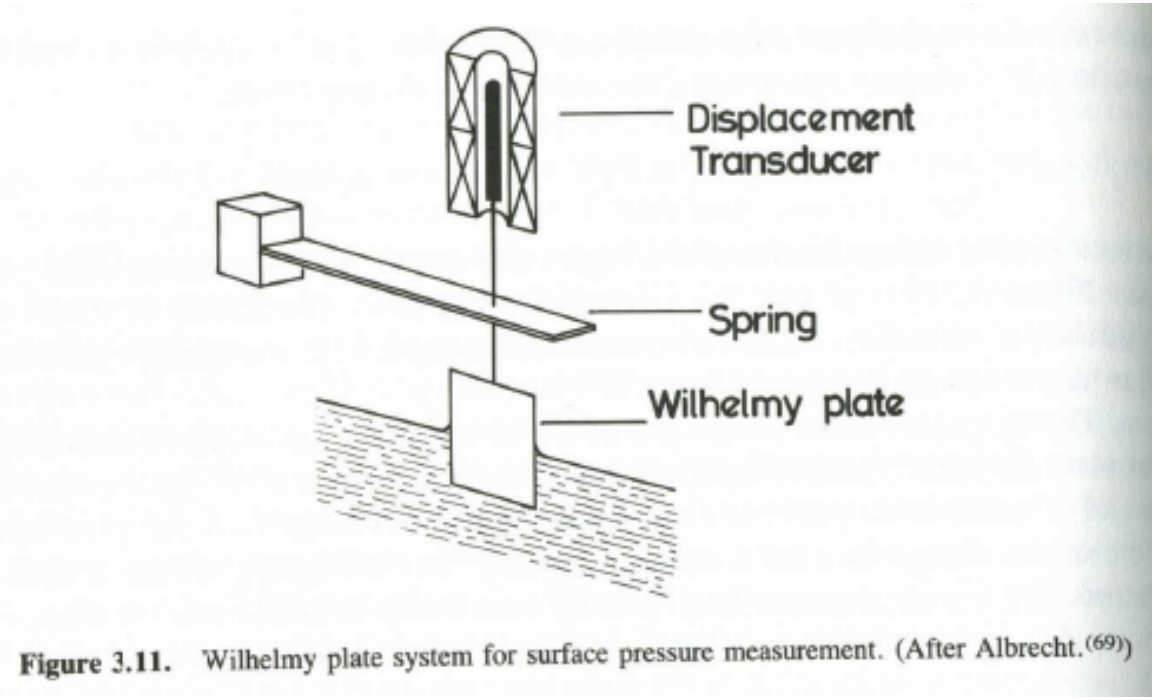

Figure 3.11. Wilhelmy plate system for surface pressure measurement. (After Albrecht.[69])

©2010 | A.J. Hart | 63